Interactions between right and left olfactory cortices *via* the anterior commissure

前交連を介した左右嗅皮質間の相互作用

菊田　周

Table of contents

Abstract

Visual and auditory systems use two sensory organs to monitor the external sensory signals. In olfactory systems, odors are inhaled through the nostrils into two segregated nasal passages and processed by two, right and left olfactory pathways. Anterior olfactory nucleus (AON) of the adult rat olfactory cortex receives excitatory axonal inputs from ipsi-lateral olfactory bulb and also receives inputs from contra-lateral olfactory cortex *via* the anterior commissure (AC), suggesting that it receives converging inputs from ipsi-lateral and contra-lateral olfactory epithelia. To study the functional interactions between right and left olfactory pathways, I recorded extracellular single unit activity of AON neurons and examined their responses to ipsi-nasal and contra-nasal stimulation with 10 odorant categories. I found 1) that about 60 % neurons in the AON received converging excitatory inputs from both olfactory epithelia, 2) that these binasal neurons were preferentially located in the deep part of the layer Ⅱ in the AON, and 3) that binasal neurons in the AON respond to ipsi-nasal and contra-nasal inputs with nearly-equivalent odorant category selectivity. Furthermore, deprivation of ipsi-nasal inputs by unilateral nostril obstruction greatly enhanced

the response to contra-lateral odor stimulation, in a reversible manner, in about 33% of AON neurons within only several minutes. In 27% of AON neurons that showed spike responses induced by the inspiration of room air, ipsi-lateral nasal obstruction initially suppressed respiration phase-locked spike discharges and, several minutes later, induced respiration phase-locked discharges with longer delays between inspiration and response. Recordings from AON neurons in rats with AC transection indicated that the resumed respiration phase-locked discharges with longer delays were mediated by the contra-lateral pathway *via* the AC. The ipsi-nasal occlusion-induced switching of nasal inputs to individual AON neurons shows that a subset of AON neurons in the adult rat has neuronal mechanisms for rapid nostril dominance plasticity, which may enable both right and left olfactory cortices to preserve their responsiveness to the external odor world, despite reciprocal changes in nasal airflow.

Introduction

Individual visual and auditory sensory systems have two sensory organs to monitor environmental cues. In visual system, binocular comparisons allow for depth perception (Barlow, 1967). In auditory system, interaural cues subserve the localization of sound sources (Knudsen at al., 1979). What is the functional significance of having two, right and left olfactory pathways?

The two nasal passages are almost completely isolated from each other and airflow through the two, right and left nasal passages is usually asymmetrical. A slight to mild inflammatory rhinitis causes one of the typical symptoms, a spontaneous alternative unilateral obstruction because of the nasal congestion. Complete or partial obstruction of a unilateral airway occurs even in normal physiological conditions, and has been reported as nasal cycle (Bojsen-moller et al., 1971; Eccles et al., 2000a). Such a collapse of a unilateral nasal airway prevents environmental odor information from reaching not only the olfactory epithelium (OE) but also the olfactory bulb (OB) on the blocked side; this occurs because the olfactory sensory neurons in the OE selectively project their axons to the ipsi-lateral (ipsi)-OB (Fig. 1) (Mori et al., 1999). The mitral and tufted cells in the OB also selectively project their axons to the ipsi-olfactory cortex (OC) (Scott

et al., 1980; Neville et al., 2004).

In the developing visual cortex, monocular deprivation leads to a functional weakening of inputs from the deprived eye and a persistent enhancement of inputs from the non-deprived eye (Hensch et al., 2005). The adult mouse visual cortex also shows a form of ocular dominance plasticity; depriving the dominant contra-lateral eye of vision leads to a persistent enhancement of the weaker ipsi-lateral eye inputs (Sawtell et al., 2003). Because of the frequent occurrence of unilateral nasal occlusion in the olfactory system, I hypothesized that when ipsi-nasal inputs are deprived by nasal occlusion, neurons in the adult rodent OC may enhance the inputs from the contra-lateral, non-occluded nose.

The anterior olfactory nucleus (AON) is found at the most rostral region of the OC. AON neurons project their axons as association fibers to the ipsi-OC, and to the contra-lateral (contra)-AON and contra-OC *via* the anterior commissure (AC) (Fig. 1) (Schoenfeld et al., 1984; Brunjes et al., 2005). It appears that the AON receives axonal inputs *via* the AC from the contra-AON or contra-OC (Haberly et al., 1978), and thus receives sensory signals from both the ipsi- and contra-OEs (Wilson et al., 1997; Lei et al., 2006). Upon ipsi-nasal obstruction, the AON may obtain external odor information from the pathway consisting of the

contra-OE, contra-OB, contra-AON/OC, and AC (blue pathway in Fig. 1).

In the present study, I recorded the single-unit spike responses of AON neurons in the brain of urethane-anesthetized rats to 10 odorant categories (Fig. 2). I observed the detailed response properties for ipsi-nasal and contra-nasal stimulation with odorants. And I analyzed the spatial distribution of AON neurons showing interactions between right and left olfactory cortices. In addition, I examined the effect of unilateral nasal obstruction on the odor response to contra-nasal stimulation.

Results

I used a stimulus panel of odors consisting of ten odorant categories for nasal stimulation (Fig. 2). I first examined whether the external nasal septum was effective for selective odorant stimulation of the unilateral OE (Fig. 3*A*). I recorded extracellular, single unit activity from mitral/tufted cells in the OB, which selectively project their axons to the ipsi-lateral OC. All the recorded mitral/tufted cells showed excitatory responses to only ipsi-lateral nasal stimulation with odorants, and not to contra-lateral stimulation (Fig. 3*B*; Table 1). This indicated that contra-lateral nasal stimulation selectively stimulated the contra-lateral OE, or, alternatively, that the amount of odorants intruding from the ipsi-lateral nasal cavity was insufficient to drive the spike responses of mitral/tufted cells beyond the stimulation threshold.

I then recorded E-E (ipsi-excitation, contra-excitation) type AON neurons (Fig. 3*C*; Fig. 4*A*) that showed excitatory responses both to ipsi-nasal and contra-nasal odor stimulation. I confirmed that obstruction of the ipsi-nostril by placement of a chitin membrane completely abolished the spike response of AON neurons to ipsi-nasal stimulation, but did not suppress their response to contra-nasal stimulation (Fig. 3*C*, upper panel). Conversely, contra-nostril

obstruction completely abolished spike responses to contra-nasal stimulation while leaving intact the response to ipsi-nasal stimulation (Fig. 3*C*, middle panel). These observations indicate the efficacy of the external nasal septum and chitin membrane for selectively stimulating only one OE.

Responses of AON neurons to ipsi-nasal and contra-nasal odor stimulation

In 56 recorded AON neurons, I analyzed 52 AON neurons that showed excitatory response to at least one odorant category among the 10 categories tested (Fig. 2). About 60% (31 neurons) of these neurons were excited by both ipsi-nasal and contra-nasal stimulation from at least one odorant category, and were thus identified as binasal E-E (ipsi-excitation, contra-excitation) type neurons (Fig.4*A* and center column in Fig. 4*B*). Figure 4*A* shows an example of excitatory responses of a binasal AON neuron to ipsi- and contra-nasal stimulation with phenol odorants. The remaining 40% of AON neurons were ipsi-nasal neurons that showed excitatory response only to ipsi-nasal stimulation (Fig. 4*B*, left column); three of these also showed suppressive responses to contra-nasal stimulation [E-I (ipsi-excitation, contra-suppression) type neurons; Fig. 5*B*]. The ipsi-nasal AON neurons received either no excitatory input from the contra-OE, or

weak contra-nasal input below the threshold needed for a spike response. I found no AON neurons that showed an excitatory response to contra-nasal stimulation and no response to ipsi-nasal stimulation (contra-nasal neurons, Fig. 4*B*).

Some AON neurons (3 cells) were suppressed by both ipsi-nasal and contra-nasal stimulation from at least one odorant category, and were thus identified as I-I type neurons (Fig. 5*D*). One cell was detected as I-0 (ipsi-suppression, contra-zero) neurons (Fig. 5*E*). Thus I divided AON neurons into five types based on the response properties; binasal E-E type, ipsi-nasal E-I type, ipsi-nasal E-0 type, I-I type and I-0 type AON neurons (Fig. 5). Because the I-I type and I-0 type neurons constitute only a small minority of the recorded AON neurons, they were excluded from the detailed analysis in the present study.

The odor-induced spike responses of most AON neurons were phase-locked with the respiration cycle (Figs. 4*A*; Fig. 6). Responses to ipsi-nasal odor stimulation occurred largely during the inspiration phase or the initial part of the expiration phase (Fig. 6*B*), while contra-nasal odor responses generally occurred during the initial or later parts of expiration (Fig. 6*C*; Fig. 7*A*). Thus, the peak of the spike response to ipsi-nasal odor stimulation in the respiration phase histogram precedes that of the response to contra-nasal stimulation. This may

occur because responses to contra-nasal stimulation are mediated by a longer pathway and a larger number of synaptic transmissions that include cortico-cortical synaptic interaction via the commissural fibers crossing the AC.

To confirm that the responses of binasal neurons to contra-nasal stimulation are mediated by the neuronal pathway traversing the AC, I surgically performed AC transection in four rats and examined the response to ipsi- or contra-lateral odor stimulation. The AON neurons in these rats indeed responded to ipsi-nasal stimulation but not to contra-nasal stimulation (Fig. 4*C*), indicating that AC mediates the sensory input from the contra-OE to the ipsi-AON.

Examination of odorant category selectivity of individual binasal neurons when odorants were introduced ipsi- or contra-nasally revealed that neurons were tuned to either a single odorant category or a specific combination of odorant categories (Fig. 8), as previously observed for neurons in the anterior piriform cortex (Yoshida et al., 2007). Surprisingly, in all 13 binasal E-E (ipsi-excitation, contra-excitation) type AON neurons examined in detail, the odorant category profile of ipsi-nasal inputs closely resembled that of the contra-nasal inputs (Fig. 8). However, for individual neurons, the contra-nasal-activating odorant categories were often a subset of the ipsi-nasal-activating odorant categories. In

addition, in most cases the ipsi-OE stimulation response was larger than the contra-OE stimulation response for odorants within the same category (Fig. 4*A*; Fig. 9; Table 1, one-way ANOVA; no significant differences among animals, paired t-test in 31 binasal neurons, $p < 0.01$). Thus, individual binasal neurons receive nearly equivalent odor signals from right and left OEs in terms of odorant category profile selectivity. In addition, the magnitude of ipsi-nasal inputs to the binasal neurons typically exceed those of contra-nasal inputs (Fig. 9). This observation of binasal neurons together with the presence of ipsi-nasal AON neurons and the absence of contra-nasal neurons indicates that most AON neurons are dominated by ipsi-nasal inputs.

Bilateral nasal stimulation with the same odorant category

In addition to spike activity for unilateral nasal stimulation with odorant category, I examined the response properties of AON neurons for bilateral concomitant nasal stimulation with the same odorant category in 5 cells. Fig. 10 shows one example that showed mixture facilitation to the bilateral nasal stimulation with the same odorant category. The cell in Fig. 10 showed excitatory responses to ipsi-nasal stimulation with ester or acid category (Fig. 10*A, D*), but

only a weak excitatory responses to contra-nasal stimulation with ester category (Fig. 10*C*) or not to contra-nasal stimulation with acid category (Fig. 10*F*). The response magnitude for bilateral nasal stimulation was about two folds larger than the summation of responses to ipsi- and contra-nasal stimulation (Fig. 10*B, E*).

Among the 5 AON neurons examined, binasal mixture facilitation was observed in 2 neurons. However, other 3 neurons did not show the clear binasal mixture facilitation. These results indicate that a subset of AON neurons shows mixture facilitation to the bilateral nasal stimulation with the same odorant category.

Spatial representation of binasal and ipsi-nasal neurons in layer Ⅱ of the AON

The major portion of the AON, pars principalis, has laminar organization and can be divided into an outer plexiform layer (layer I), a cell layer (layer Ⅱ) and layer Ⅲ based on Nissl stains (Fig. 11*A*). I examined the laminar distribution of the 44 neurons recorded in the AON (binasal E-E type; 32 cells, ipsi-nasal E-0 type; 12 cells). Most of the AON neurons [84%, 37 cells; binasal E-E type (26 cells), ipsi-nasal E-0 type (11 cells)] were recorded from layer Ⅱ. I further examined the sublayer specific distributions of the 37 AON neurons recorded in

the layer Ⅱ. The layer Ⅱ is divided into two sublayers; superficial part of the layer Ⅱ (layer Ⅱa) and deep part of the layer Ⅱ (layer Ⅱb). Fig 11*C* indicates a representative coronal section through the AON with dot marks that shows recorded sites. Most of the binasal E-E type neurons (8 cells out of 9 binasal E-E type neurons, red dots) were recorded from layer Ⅱb. In contrast, all the ipsi-nasal E-0 type neurons (2 cells, blue dots) were recorded in the layer Ⅱa.

Among 37 AON neurons examined (binasal E-E type neurons; 26 cells, ipsi-nasal E-0 type neurons; 11 cells, 7 slices), ipsi-nasal E-0 type neurons were mostly located in layer Ⅱa (Fisher's exact probability test, probability of the layer Ⅱa-specific distribution in the 11 ipsi-nasal E-0 type neurons, $p<0.05$). Binasal E-E type neurons were found in both layer Ⅱa and layer Ⅱb with a tendency to distribute significantly more in layer Ⅱb (Fig. 11D) (Fisher's exact probability test, probability of the sublayer-specific distribution in the 26 binasal E-E type neurons, $p<0.05$). These results suggest that there is a sublayer-specific processing of uninasal and binasal odor information.

Deprivation of ipsi-nasal inputs rapidly enhances contra-nasal inputs to AON neurons

I next examined the effect of dominant ipsi-nasal input deprivation caused by ipsi-nostril obstruction on the response of individual AON neurons to contra-nasal stimulation. When both nostrils were left open, the cell pictured in Fig. 12*A* was observed to respond strongly to ipsi-OE stimulation with "ether" category odorants, but did not respond to contra-OE stimulation with the same odorants. When the ipsi-lateral nostril was blocked by placement of the chitin membrane at time 0 (filled triangle in Fig. 12*A*), the cell remained unresponsive to contra-OE stimulation for about 200 sec, and then began responding strongly (Fig. 12*A*, c). Upon re-opening of the ipsi-nostril (open triangle in Fig. 12*A*), the cell rapidly lost its heightened responsiveness to contra-OE stimulation. After subsequent, repeated obstruction of the ipsi-nostril (610 sec after the first obstruction, filled triangle), the cell again responded strongly to contra-OE stimulation, approximately 160 sec later.

A similar analysis of 27 AON neurons which responded strongly to ipsi-nasal input of an odorant category but more weakly or not at all to contra-nasal input of the same category revealed that 33% (9 neurons) showed markedly enhanced

responsiveness to contra-nasal input several minutes after ipsi-nostril obstruction. However, the remaining 18 AON neurons did not show enhanced responses to contra-nasal input, even several minutes following ipsi-nostril closure. These results indicate that deprivation of ipsi-nasal inputs causes a marked enhancement of contra-nasal inputs in a subset of AON neurons.

To exclude the possibility that repetitive odor stimulation of the contra-OE causes the marked enhancement of the contra-nasal inputs to the ipsi-AON neurons, I recorded 26 AON neurons that responded to ipsi-nasal odor stimulation and repetitively stimulated the contra-OE without the ipsi-nasal obstruction. In all the neurons, the repetitive odor stimulation for 5 min (at the rate of once per 25 sec) did not cause the heightened responsiveness to the contra-nasal odor stimulation. Furthermore, I observed in 3 neurons (among 15 neurons examined) that the subsequent ipsi-nasal obstruction caused a marked enhancement of the responses to the contra-OE stimulation with odorants (Fig. 13). These results indicate that the ipsi-nasal obstruction but not the repetitive contra-OE stimulation causes the marked enhancement of the contra-nasal inputs in a subset of AON neurons (Fisher's exact probability test, probability of recording neurons that shows increased responses to the contra-nasal odor stimulation; 9 cells out of 27

cells examined with ipsi-nasal obstruction, 0 cells out of 26 cells examined without ipsi-nasal obstruction, $p<0.01$).

In the absence of odor stimulation, about 27% (119 out of 440 cells recorded) of AON neurons showed respiration phase-locked spike discharges which were presumably induced by room air odorants or periodic mechanical stimulation of the olfactory sensory neurons due to nasal airflow (Grosmaitre et al., 2007). These respiration-related discharges occurred at the late phase of inspiration or the initial phase of expiration (Fig. 7*B*; Fig. 12*B*). The effect of ipsi-nasal obstruction was examined in 63 AON neurons that showed room air-induced respiration phase-locked discharges. In all of these AON neurons, ipsi-nasal obstruction initially completely suppressed respiration phase-locked spike discharges, which suggests that respiration phase-locked inputs from the contra-OE were absent or below the threshold for inducing spike responses, just after ipsi-nasal obstruction. However, 22 to 292 sec (138±25 sec, mean±SD, n=17) after nostril obstruction, about 27% (17 of the 63 cells) began to show robust respiration phase-locked spike discharges with longer delays between inspiration and response (Fig. 7*B*; Fig. 12*B*; Fig. 14*B*; Table 2). Activity exhibiting longer delays suggests that the resumed respiration phase-locked activity was induced by the remaining inputs

from the contra-OE.

To examine this hypothesis, I studied the effect of ipsi-nasal obstruction on the respiration phase-locked activity of AON neurons in rats with AC transection (3 rats). In 18 AON neurons which showed respiration phase-locked spike discharges, ipsi-nasal obstruction completely abolished the respiration phase-locked spike discharges throughout the 5 minute period of nostril obstruction. The absence of resumed respiration phase-locked activity in these rats indicates that the resumed respiration phase-locked inputs observed in rats with intact AC are mediated *via* the AC (Fisher's exact probability test, probability of recording neurons that show resumed phase-locked firing after ipsi-nasal obstruction; 17 cells out of 63 cells examined (~27%) in the AC intact group, and 0 cells out of 18 cells (0%) in the AC transected group, $p<0.01$)

The increased response of the AON neurons to contra-nasal inputs after ipsi-nasal blockage may be due to the plastic mechanism of the neuronal pathway from the contra-OE *via* contra-OB, contra-AON/OC to the ipsi-AON. However, there remains the possibility that the increased response of AON neurons is simply due to increased air flow in the contra-nasal passage because of the blocking of the ipsi-nasal passage. To examine the latter possibility, I recorded responses of

AON neurons before and after ipsi-lateral nostril closure, while simultaneously monitoring the air flow in the contra-nostril by using a thermocouple. I found that the airflow rate in the contra-nostril increased at the onset of ipsi-nasal obstruction; however, the airflow was unchanged at the time the neurons suddenly developed enhanced responsiveness to contra-OE stimulation (Fig. 14). Although the lack of temporal correlation between the onset of the increased airflow and the onset of the increased response does not necessarily rule out the possibility of the causal relationship, the results indicate that the increased responses cannot be explained solely by the increased airflow. These observations suggest that the central olfactory system contains a neuronal mechanism that switches nasal inputs to the contra-OE when ipsi-nasal inputs are blocked.

Discussion

The present results showed that in binasal E-E (ipsi-excitation, contra-excitation) type AON neurons, odorant category selectivity of contra-nasal inputs closely resembled that of the ipsi-nasal inputs. Individual binasal neurons thus receive similar odor information from the ipsi-nasal pathway and the contra-nasal pathway (cf. Fig. 1; Fig. 15), suggesting the presence of the coordinated neuronal connections between ipsi-lateral and contra-lateral olfactory cortices. The binasal AON neurons may be involved in the neuronal mechanisms for the transfer of ipsi-nasal olfactory information to the contra-lateral OC *via* the AC (Fig. 15) (Kucharski et al., 1987).

Convergence of similar sensory information upon individual neocortical neurons from right and left sensory organs has been reported in visual and auditory systems (Hubel et al., 1962; Middlebrooks et al., 1980). Detection by these sensory cortices of subtle signal differences between bilateral sensory organs facilitates computation of visual depth and localization of a sound source, respectively (Barlow et al., 1967; Knudsen et al., 1979). In auditory system, mammals have two specialized cues, interaural time differences and interaural intensity differences (IIDs) to localize sound source. IIDs are first coded by

neurons in the lateral superior olive (LSO). The neurons in the LSO receive its principal excitatory inputs from the ipsilateral ear and inhibitory inputs from the contralateral ear (Park et al., 1997). The olfactory system also has the ability to localize the odor source (Rajan et al., 2006; Bekesy et al., 1964; Porter et al., 2005). By analogy with the auditory system (Konishi, 1983), internostril intensity differences might be a candidate for stereo cues in the AON. Thus, one possible function of the convergence of nearly equivalent olfactory signals from bilateral OEs is to detect the subtle difference of signals from the two OEs, which may be the role played by subpopulations of E-E (ipsi-excitation, contra-excitation) type and E-I (ipsi-excitation, contra-suppression) type AON neurons. Another important function of equivalent convergence is to maintain a reserve of sensory input, so that in the event that one sensory organ is temporarily not functional, the brain can monitor the external world through the remaining intact sensory organ.

My result indicated that a majority of ipsi-nasal E-0 (ipsi-excitation, contra-zero) type AON neurons were located in the superficial part of the layer Ⅱ, whereas binasal E-E (ipsi-excitation, contra-excitation) type AON neurons tended to distribute in the deep part of the layer Ⅱ. These results suggest that a sublayer-specific processing of uninasal and binasal odor information.

Previous reports indicate that the superficial part of the layer Ⅱ contains extraverted pyramidal cells, semilunar type, with no basal dendrites, whereas the deep part of the layer Ⅱ contains large pyramidal cells with some ascending apical and numerous basal dendrites (Valverde F et al., 1989). Thus, sublayer-specific distribution of E-E type and E-0 type AON neurons correlate with the sublayer-specific distribution of the two morphological types of AON neurons.

To examine the morphology, I injected dextran-amine dye into a binasal E-E type AON neuron using the electrophoration method (Fig. 16). This binasal E-E type neuron showed a typical pyramidal neuron morphology, whose somata was located at the border between layer Ⅱ a and Ⅱ b. Further morphological analysis is necessary to reveal the possible correlation between the cell types, binasal E-E type or ipsi-nasal E-0 type neurons, and their morphology.

My result showed that in the binasal E-E (ipsi-excitation, contra-excitation) type AON neurons, ipsi-nasal inputs exceeded contra-nasal inputs in magnitude. Thus, the activity of AON neurons is ordinarily dominated by ipsi-nasal inputs. In addition, I showed that ipsi-nostril obstruction rapidly enhanced, within several minutes, the contra-nasal input of a subset of AON neurons in a reversible manner. These results indicate a novel form of binostril competition in the adult OC.

Congestion of nasal mucosa is thought to be a necessary step for mucous clearance (Eccles et al., 2000b); however, the process inevitably alters nasal airflow and the concomitant activity of the left and right OEs. To cope with the reciprocal change in OE activity, the central olfactory system may have evolved a homeostatic plasticity mechanism of neural circuits for rapidly adjusting the magnitude of contra-nasal inputs based on the magnitude of ipsi-nasal inputs, such that at least a subset of AON neurons can continue to respond to external odors. As a first step to understand the plasticity of the central olfactory system, I examined the change in the contra-nasal input following a complete obstruction of the ipsi-nasal passage. Because the natural nasal obstruction is almost always a partial obstruction, further experiments are necessary to examine the responses to contra-nasal stimulation following partial and graded obstructions of the ipsi-nasal passage.

A global homeostatic mechanism that provides stability to neuronal networks has been reported to work in the juvenile mouse visual cortex during ocular dominance plasticity (Mrsic-Flogel et al., 2007). Monocular deprivation results in decreased deprived-eye inputs, increased non-deprived eye inputs in neurons that receive binocular inputs, and increased deprived-eye responses in neurons devoid

of non-deprived eye inputs (Mrsic-Flogel et al., 2007), indicating that the response adjustment effectively preserves the net visual drive for individual neurons. I speculate that a similar homeostatic plastic mechanism may work in the adult olfactory system to preserve the net olfactory drive for each AON neuron. A previous study showed that unilateral naris obstruction for more than 30 days enhances the intracortical association fiber input to the olfactory cortex of the adult rat (Best et al., 2003). Unilateral nostril obstruction for 5 days causes down-regulation of the NMDA receptor NR2B subunit and phospho-CREB, specifically in layer Ⅱb pyramidal cells of the mouse OC (Kim et al., 2006). These results raise the possibility that similar changes may occur in the AON during rapid compensatory switching of binasal inputs.

One possible mechanism underlying the ipsi-nostril obstruction induced boost-up of contra-nasal inputs might be associated with the changes in the cholinergic modulatory inputs to the ipsi-AON. The cholinergic system has neuromodulatory effects on broad region of the brain including AON, but targets its influence to presynaptically associational fiber excitatory synapses (Hasselmo and Bower, 1992). In addition, the activity of cholinergic neurons in the horizontal limb of diagonal band of Broca can be modulated by the afferent olfactory sensory

inputs (Chritiane and Hasselmo, 2000). These raise a possibility that, when ipsi-nostril was obstructed, cholinergic modulatory inputs might be reduced depending on the afferent nasal inputs. Thus when the afferent inputs to the ipsi-AON were diminished by the ipsi-nostril obstruction, low levels of cholinergic inputs presynaptically might release the partial suppression of glutamatergic inputs from contra-OC to the ipsi-AON neuron via the AC, resulting in the heightened contra-nasal inputs to the ipsi-AON neuron. Further work is necessary to elucidate the cellular, synaptic, and molecular mechanisms of AON rapid plasticity.

It remains to be determined whether ipsi-nasal obstruction causes any change in the responses of mitral cells in the contra-OB to the contra-nasal odor stimulation. If there are changes in the mitral cell responses, future studies should address the question to what extent the plasticity of AON neurons is due to the altered outputs of mitral cells in the ipsi- and contra-OBs.

A characteristic feature of mono-nasal deprivation-induced nasal dominance plasticity is its extreme rapidness; the increase in responsiveness to contra-nasal inputs occurs within several minutes following the onset of ipsi-nostril closure. This is in striking contrast to the visual and auditory systems which require

long-term deprivation of unilateral sensory input to induce the plastic change of central neuron responses to input from the non-deprived sensory organ. In the adult mouse visual cortex, more than 2 days of monocular deprivation is required to induce homeostatic plastic changes (Goel et al., 2007). In the inferior colliculus of the adult ferret auditory system, one day removal of input from the dominant, excitatory contra-lateral ear is needed to induce enhanced excitation from the ipsi-lateral ear (McAlpine et al., 1997). The rapid nature of the mono-nasal deprivation-induced nasal dominance plasticity in the AON of adult rats provides a useful model system with greater experimental tractability for analyzing the cellular and molecular mechanisms of experience-dependent cortical plasticity in the adult brain.

Rapid switching of binasal inputs to a subset of AON neurons may enable both right and left olfactory cortices to continuously monitor the external odor world despite unilateral and reciprocal obstruction of the nasal airflow. This objective is further facilitated by the fact that individual neurons of this subset obtain similar olfactory information from the ipsi- and contra-OEs.

Material and Methods

Animals

All experiments were performed in accordance with the guidelines of the Physiological Society of Japan and were approved by the experimental animal research committee of the University of Tokyo. Wistar rats (male, 280 – 350 g: Japan SLC, Shizuoka, Japan) were anesthetized with urethane (1.2 g/kg) (Nagayama et al., 2004) and placed in a stereotaxic apparatus (SR-6R, Narishige, Tokyo, Japan). Body temperature was maintained at 37.5 °C by a homeothermic heat pad system (MK-900, Muromachi Kikai, Tokyo, Japan). Respiration was monitored by measuring chest movement with a strain gauge (TR-651T; Nihon Kohden, Tokyo, Japan), or by examining nasal airflow with a thermistor (BAT-12, Physitemp Instruments, USA). The thermistor probe was placed in the nasal vestibule contra-lateral to the recording side, without touching the nasal mucosa. We subjected seven rats to AC transection using a miniature edge blade (501251, World Precision Instruments, USA). The success of the AC transection in each rat was confirmed histologically after the experiment was completed.

Odor stimulation

For uni-nasal odor stimulation, thermoplastic material was used to construct an external nasal septum which fit the external shape of the rat nose. In addition, one nostril was obstructed by pasting on a chitin membrane (0.5 cm in diameter and moisturized with saline), which allowed non-invasive obstruction or re-opening of one nostril (Fig. 2*C*). To stimulate the OE with each odorant category, we first used the method of placing test tubes containing diluted odorants (5% in odorless mineral oil) in front of a nostril at a distance of 2 cm. After monitoring the odorant category selectivity of individual AON neurons, we then examined the effect of nostril obstruction using a custom made air-dilution olfactometer fitted with Teflon tubing, controlled by a program written in Labview software (National Instruments, USA). Odorant vapor was produced by flowing clean air through disposable glass microfiber syringe filters (2.7 μm pore size, Whatman) loaded with 30 μl liquid odorant. Each odorant stream (300 ml/min) was mixed with a clean air stream (200 ml/min) to produce a total flow rate of 500 ml/min in a Teflon tube. The outlet of this tube was placed 2 cm in front of the ipsi-nostril (recorded side) or the contra-nostril. An exhaust pipe was placed over the head of the rat to suck up any stray odorants.

Odorants

Ten odorant categories (sulfide, ester, terpene hydrocarbon, acid, ether, ketone, aldehyde, alcohol, lactone and phenol) were used (Fig. 2). A mixture of five representative odorants was used for stimulation with an individual category. In some experiments, stimulation with individual component odorants was also performed. The odorants were a kind gift from T. Hasegawa (Tokyo, Japan), or were purchased from Sigma-Aldrich (St. Louis, MO), Tokyo Kasei Organic Chemicals (Tokyo, Japan), or Nacalai tesque (Kyoto, Japan).

Electrophysiology

For extracellular single-unit recordings, a small hole was made in the skull above the AON (3.8–4.7 mm anterior to the bregma, 1.7–2.3 mm lateral from the midline). A glass micropipette (10–20 MΩ) filled with 2% Chicago Sky Blue 6B (Tocris Bioscience, Bristol, UK) in 0.5 M sodium acetate was inserted vertically into the pars principalis of the AON (Brunjes et al., 2005).

After single-unit recordings, a negative current was applied so that the recorded sites could be marked by the dye (20 μA, 2 min). The dye-marked sites were examined histologically. The signals of single-unit activities were amplified

(AB-610J, Nihon Kohden, Tokyo, Japan), filtered (150–10 kHz) (EW-610J, Nihon Kohden), and stored on a computer.

For extracellular single-unit recordings from OB neurons (two rats), the bone above the OB and lateral olfactory tract (LOT) was removed by using a dental drill. A concentric, bipolar stainless electrode (EKC - 5002K, Eikoh Kagaku, Tokyo, Japan) was inserted into the LOT (3.0 mm anterior from the bregma, 3.5 mm lateral from the midline, ~ 6 mm from the brain surface) for electrical stimulation (once every 3 sec, 100 μsec in duration). A glass micropipette (1–5 MΩ) filled with 4 M NaCl was inserted into the OB. Single-unit activities were recorded exclusively from the external plexiform layer or mitral cell layer.

For multi-site single-unit recordings from AON neurons, a silicon-based stereotrode (16 or 32 channels, Neuro Nexus Technologies, USA) was used. Recording sites in the probe were spaced at 100 μm intervals. After removing the skull and dura matter, the stereotrode was inserted into the AON through the frontal cortex. Monitoring of the LOT-evoked local field potentials indicated that most of the recording sites were placed at layer II of the AON, pars principalis. Signals were amplified (AB-610 J, Nihon Koden, Japan), filtered (150 Hz–10

kHz) (EW-610J, Nihon Koden, Japan), digitized (Power 1401, CED, UK) and stored on a computer. In recordings made with the stereotrode, single units were isolated from recorded signals in each recording site by using template matching and principal component analysis methods. Raster plots and peri-stimulus time histograms were obtained as described previously (Nagayama et al., 2004). In the raster plots, trials are shown in chronological order from bottom to top. After the recording session, small lesions were made by current injections (5 μA during 5 sec) for later histological examination of the recorded sites.

For electro-encephalogram (EEG) recording, a stainless-steel screw was threaded into the bone above the occipital cortex. Another screw was threaded into the bone above the cerebellum, and used as a reference.

Analysis

Spike2 software (Cambridge Electronic Design, Cambridge, UK) was used offline to analyze spike firing rate, and to a make raster representations, peri-stimulus time histograms (1 bin = 0.1 sec in Figs. 2 and 3, 1 bin = 0.3 sec in Fig. 6 and supplemental Fig. 1) and respiratory phase histograms (one respiration = 24 bins) of spikes. The response magnitude (R.M.) to odor stimulation (Fig. 6

and Fig. 7) was calculated by subtracting the number of spikes during the 3 sec period immediately prior to odor stimulation from the number of spikes observed during the 3 sec period of odor stimulation, and was expressed as firing rate (number of spikes/sec).

In rats under urethane anesthesia, the neocortical EEG alternates between the slow-wave state and the fast-wave state (Murakami et al., 2005). To minimize the influence of state-dependent sensory gating, all spike responses to odorants were obtained during the fast-wave state.

Based on responses to odor stimulation, we classified AON neurons into two types: binasal neurons and ipsi-nasal neurons. Binasal neurons showed excitatory spike responses to both ipsi-OE and contra-OE stimulation with at least one odorant category. Thus, I designated these neurons binasal excitation-excitation (E-E) type neurons. Most of the ipsi-nasal neurons showed excitatory spike response to ipsi-OE stimulation, but did not respond to contra-OE stimulation. Some of the ipsi-nasal neurons showed an excitatory spike response to ipsi-OE stimulation and a suppressive response to contra-OE stimulation. These neurons were designated excitation-inhibition (E-I) type neurons. Some neurons that shows suppressive responses both to ipsi-nasal and contra-nasal stimulation with

odorants or only to ipsi-nasal stimulation with odorants, but not to contra-nasal stimulation with odorants were also observed. I defined these neurons as I-I (ipsi-suppression, contra-suppression) type and I-0 (ipsi-suppression, contra-zero) type neurons, respectively. However, I exclude these neurons that receive suppressive response to ipsi-nasal stimulation with odorants from the analysis of population data because of the difficulty in accurately estimating the suppressive responses to nasal stimulation. Furthermore, I defined a binasal mixture facilitation as follows; the response magnitude for bilateral concomitant nasal stimulation exceeded more than two or more fold the summation of responses magnitude for ipsi- and contra-nasal stimulation with at least one odorant category.

To estimate the degree of similarity between odorant category selectivity of ipsi-nasal input and that of contra-nasal input, we counted for each neuron the number of odorant categories (among 10 categories examined) that induced matched responses between ipsi-OE stimulation and contra-OE stimulation.

For each odorant category, the bi-lateral match response was determined as +1 matched; excitatory ipsi-response plus excitatory contra-response, or no ipsi-response plus no contra-response or as 0 non matched; excitatory

ipsi-response plus no contra-response, or no ipsi-response plus excitatory contra-response). For each cell, the number of bilateral category matches was determined by summating all +1 matched responses. The averaged number of the bi-lateral category matches (n = 13 cells) was then calculated (Fig. 8; Table 1).

For 31 binasal neurons, the most effective odorant category for activating individual neurons was determined. In each of the binasal neurons, we compared the averaged magnitude of responses to ipsi-OE stimulation of the most effective odorant category with that of responses to contra-OE stimulation of the same category. The difference in the averaged magnitude of responses between ipsi-OE stimulation and contra-OE stimulation was statistically examined using paired t-test (significant level, $p < 0.05$) (Fig. 9).

Stimulation of the OEs with each odorant category was performed at least three times for each OE (ipsi- or contra-OE). An excitatory spike response was defined as a significant increase (two or more fold) in the averaged firing rate during the 3 sec period of odor stimulation, as compared to that during the 3 sec period immediately prior to odor stimulation. A suppressive spike response was defined as a significant decrease (half or less) in the averaged firing rate during the 3 sec period of odor stimulation, as compared to that during the 3 sec period

immediately prior to odor stimulation. Stimulation of the OEs with each odorant category was performed at least three times for each OE (ipsi- or contra-OE).

Histology

After electrophysiological experiments were completed, animals were deeply anesthetized with urethane and perfused with 0.9% NaCl solution and then 4% paraformaldehyde (PFA) in phosphate buffer (PB, pH 7.4). The brains were post-fixed in 4% PFA in PB at 4 °C overnight. Coronal sections (50 μm thick) were cut on a microtome (VT1000s, Leica, Tokyo, Japan), mounted onto glass slides, and stained with cresyl violet. The dye-marked spots or small lesions made by current injections in the AON were visualized by using a microscope (MZ16FA, Leica). Locations of the recorded sites were reconstructed by referring to the dye mark or small lesions.

To visualize the morphology of AON neurons, I used fine glass micro-pipettes containing 4% biotinylated dextran amine dissolved in a salt solution. I injected the dye into the recorded AON neuron using the electrophoration method (Pinault, 1996). After recording the binasal E-E type AON neuron, Positive-current pulses

(< 10nA) were injected for 20 min through the micropipette to electrophorate the membrane of the recorded neuron. Six hr after the injection, the rat received an overdose of urethane and were transcardially perfused first with 0.9% NaCl solution and then 4% PFA in PB. The brains were post-fixed in 4% PFA in PB at 4 °C overnight. Coronal sections (50 μm thick) were cut and mounted onto glass slides. They were then thoroughly washed in PB before being incubated with avidin-biotin-peroxidase complex for 2 hr. The injected tracer could then be revealed with the appropriate substrate (H_20_2) and chromogen (3,3'-diaminobenzidine tetrahydrochloride) (Horikawa et al., 1988). Then, the sections were stained with Neutral red.

References

Barlow HB (1967) The neural mechanism of binocular depth discrimination. J Physiol 193:327–342.

Bekesy GV (1964) Olfactory analogue to directional hearing. J Appl Physiol 19:369-373.

Best AR, Wilson DA (2003) A postnatal sensitive period for plasticity of cortical afferents but not cortical association fibers in rat piriform cortex. Brain Res 961:81-87.

Bojsen-moller F, Fahrenkrug J (1971) Nasal swell-bodies and cyclic changes in the air passage of the rat and rabbit nose. J Anat 110:25-27.

Brunjes PC, Illig KR, Meyer EA (2005) A field guide to the anterior olfactory nucleus (cortex). Brain Res Rev 50:305-335.

Chritiane L, Hasselmo ME (2000) Neural activity in the horizontal limb of the diagonoal band of Broca can be modulated by electrical stimulation of the olfactory bulb and cortices in rats. Neuroscience letters 282:157-160.

Eccles RB (2000a) Nasal airflow in health and disease. Acta Otolaryngol 120:580-595.

Eccles RB (2000b) The nasal cycle in respiratory defence. Acta Otorhinolaryngol

Belg 54:281-286.

Goel A, Lee HK (2007) Persistence of experience-induced homeostatic synaptic plasticity through adulthood in superficial layers of mouse visual cortex. J Neurosci 27:6692-6700.

Grosmaitre X, Santarelli LC, Tan J, Luo M, Ma M (2007) Dual functions of mammalian olfactory sensory neurons as odor detectors and mechanical sensors. Nat Neuroscience 10:348-354.

Haberly LB, Price JL (1978) Association and commissural fiber systems of the olfactory cortex of the rat: II Systems originating in the olfactory peduncle. J Comp Neurol 178:781-808.

Hasselmo ME, Bower JM (1992) Cholinergic suppression specific to intrinsic not afferent fiber synapses in rat piriform (olfactory) cortex. J Neurophysiol 67:1222-1229.

Hensch TK (2005) Critical period plasticity in local cortical circuits. Nat Rev Neurosci 6:877-888.

Horikawa. K and Armstrong WE (1988) A versatile means of intracellular labeling: injection of biocytin and its detection with avidin conjugates. J Neurosci Methods 25:1-11.

Hubel DH, Wiesel TN (1962) Receptive fields, binocular interaction and functional architecture in the cat's visual cortex. J Physiol 160:106-154.

Kim HH, Puche AC, Margolis FL (2006) Odorant deprivation reversibly modulates transsynaptic changes in the NR2B-mediated CREB pathway in mouse piriform cortex. J. Neusosci 26:9548-9559.

Konishi M (1983) Coding of auditory space. Annu. Rev. Neurosci 26:31-55.

Knudsen EI, Konishi M (1979) Mechanisms of sound localization in the barn owl. J Comp Physiol 133:13–21.

Kucharski D, Hall WG (1987) New routes to early memories. Science 238: 786-788.

Lei H, Mooney R, Katz LC (2006) Synaptic integration of olfactory information in mouse anterior olfactory nucleus. J Neurosci 26:12023-12032.

McAlpine D, Martin RL, Mossop JE, Moore DR (1997) Response properties of neurons in the inferior colliculus of the monaurally deafened ferret to acoustic stimulation of the intact ear. J Neurophysiol 78:767-779.

Middlebrooks JC, Dykes RW, Merzenich MM (1980) Binaural response-specific bands in primary auditory cortex (AI) of the cat: Topographical organization orthogonal to isofrequency contours. Brain Research 181:31-48.

Mori K, Nagao H, Yoshihara Y (1999) The olfactory bulb: coding and processing of odor molecule information. Science 22:711-715.

Mrsic-Flogel TD, Hofer SB, Ohki K, Reid RC, Bonhoeffer T, Hübener M (2007) Homeostatic regulation of eye-specific responses in visual cortex during ocular dominance plasticity. Neuron 54:961-972.

Murakami M, Kashiwadani H, Kirino Y, Mori K (2005) State-Dependent Sensory Gating in Olfactory Cortex. Neuron 46:285-296.

Nagayama S, Takahashi YK, Yoshihara Y, Mori K (2004) Mitral and tufted cells differ in the decoding manner of odor maps in the rat olfactory bulb. J Neurophysiol 91:2532–2540.

Neville KR, Haberly LB (2004) in The Synaptic Organization of the Brain, ed Shepherd GM (Oxford Univ. Press, New York), pp 415-454.

Park TJ, Monsivais P, Pollak GD (1997) Processing of interaural intensity differences in the LSO: role of interaural threshold differences.

J Neurophysiol 77:2863-78.

Pinault D (1996) A novel single-cell staining procedure performed in vivo under electrophysiological control: morpho-functional features of juxtacellularly labeled thalamic cells and other central neurons with biocytin or Neurobiotin.

J Neurosci Methods 65:113-136.

Porter J, Anand T, Johnson B, Khan RM, Sobel N (2005) Brain mechanisms for extracting spatial information from smell. Neuron 18:581-592.

Rajan R, Clement JP, Bhalla US (2006) Rats smell in stereo. Science 311:666-670.

Sawtell NB, Frenkel MY, Philpot BD, Nakazawa K, Tonegawa S, Bear MF (2003) NMDA receptor-dependent ocular dominance plasticity in adult visual cortex. Neuron 38:977–985.

Schoenfeld TA, Macrides F (1984) Topographic organization of connections between the main olfactory bulb and pars externa of the anterior olfactory nucleus in the hamster. J Comp Neurol 227:121-135.

Scott W, McBride RL, Schneider SP (1980) The organization of projections from the olfactory bulb to the piriform cortex and olfactory tubercle in the rat. J Comp Neurol 194:519-534.

Valverde F, Lopes-mascaraque L, De Carlos JA (1989) Structure of the nucleus olfactorius anterior of the hedgehog. J Comp Neurol 279:581-600.

Wilson DA (1997) Binaral interactions in the rat piriform cortex. J Neurophysiol 78:160-169.

Yoshida I, Mori K (2007) Odorant category profile selectivity of olfactory cortex neurons. J Neurosci 27:9105-9114.

Acknowledgments

I sincerely thank my research advisors, Professor Kensaku Mori (Department of Cellular and Molecular Physiology) and Professor Tatsuya Yamasoba (Department of Otolaryngology) for their continuous encouragement, valuable advice and helpful discussions. And, I would like to express my appreciation to Dr. Hideki Kashiwadani for his various technical comments and discussions. Finally, I would like to acknowledge the members of the Departments of Otolaryngology and Cellular and Molecular Physiology for useful discussion.

Figure Legends

Fig. 1. Neuronal pathways from the ipsi-lateral olfactory epithelium (Ipsi-pathway) and contra-lateral olfactory epithelium (contra-pathway) to the anterior olfactory nucleus (AON).

Single-unit recordings (shown by a micropipette) were obtained from AON neurons in the animal's right olfactory cortex (OC). Shown are schematic depictions of the ipsi-nasal pathway (Ipsi-OE→Ipsi-OB→Ipsi-AON) (red), and the contra-nasal pathway (contra-OE → Contra-OB → Contra-AON/OC → Ipsi-AON) (blue) to the AON. Connection between ipsi- and contra-AONs is either monosynaptic (as shown here) or polysynaptic (not shown). AC, anterior commissure; OE, olfactory epithelium.

Fig. 2. Panel of ten odorant categories used for odor stimulation experiments.

Each odorant category consisted of five different components (①-⑤).

Fig. 3. Experimental procedure used for selective unilateral OE stimulation.

A, Schematic depiction of the unilateral OE stimulation method. An external nasal

septum made of thermoplastic material was used to separate the space in front of the right nostril from that of the left nostril. In some experiments, a chitin membrane (black disk) was also pasted onto one of the nostrils.

B, Mitral/tufted cells in the OB showed an excitatory response to ipsi-OE stimulation only. Raster representation and peristimulus time histograms of the spike response of a mitral/tufted cell to ipsi-OE (upper left, black) and contra-OE (upper right, gray) stimulation are shown. F.R., firing rate. The bottom histogram shows the number of ipsi-nasal neurons, binasal E-E (ipsi-excitation, contra-excitation) type neurons and contra-nasal neurons that were detected in the OB.

C, Excitatory spike responses of an AON neuron to ipsi-nasal (left column) and contra-nasal (right column) odor stimulation in a rat whose nostrils were subjected to unilateral nostril obstruction with a chitin membrane (upper and middle), or were both open. Ipsi-nostril obstruction selectively abolished responsiveness to ipsi-OE stimulation (upper left) while contra-nostril obstruction selectively abolished responsiveness to contra-OE stimulation (middle right), while leaving intact the response to OE stimulation in the non-occluded side.

Fig. 4. AON neurons receive contra-nasal inputs *via* anterior commissure.

A, Spike responses of a binasal (E-E type) AON neuron to ipsi-nasal (upper left, black bar) and contra-nasal (upper right, gray bar) odor stimulation. Shown are a raster representation of the spike responses (middle) and peristimulus time histograms (bottom). Bar, duration of odor stimulation (phenol category, 3 sec). The ascending and descending phases of the trace in the respiration monitor (Resp.) indicate inspiration and expiration, respectively.

B, C, The numbers of ipsi-nasal, binasal (E-E type), and contra-nasal neurons in the AONs of (***B***) control rats (with intact AC) and (***C***) AC-transected rats.

Fig. 5. Five types of response properties of the AON neurons.

A, Spike responses of a binasal E-E type AON neuron to ipsi-nasal (left, red bar) and contra-nasal (right, blue bar) odor stimulation (phenol category, 3 sec). Shown are a raster representation of the spike responses and peristimulus time histograms. The binasal E-E type AON neuron showed excitatory responses to both ipsi-nasal (left) and contra-nasal odor stimulation (right). Colored bar; duration of odor stimulation (phenol category, 3 sec).

B, Spike responses of an ipsi-nasal E-I type AON neuron to ipsi-nasal (left, red

bar) and contra-nasal (right, blue bar) odor stimulation (ether category, 3 sec). The ipsi-nasal E-I type AON neuron showed excitatory response to ipsi-nasal stimulation (left) and suppressive response to contra-nasal stimulation (right).

C, Spike responses of an ipsi-nasal E-0 type AON neuron to ipsi-nasal (left, red bar) and contra-nasal (right, blue bar) odor stimulation (sulfide category, 3 sec). The ipsi-nasal E-0 type AON neuron showed excitatory response only to ipsi-nasal stimulation (left).

D, Spike responses of an I-I type AON neuron to ipsi-nasal (left, red bar) and contra-nasal (right, blue bar) odor stimulation (ether category, 3 sec). The I-I type AON neuron showed suppressive response to both ipsi-nasal (left) and contra-nasal stimulation (right).

E, Spike responses of an I-0 type AON neuron to ipsi-nasal (left, red bar) and contra-nasal (right, blue bar) odor stimulation (ester category, 3 sec). The I-0 type AON neuron showed suppressive response only to ipsi-nasal stimulation (left).

Fig. 6. Respiration phase histograms of spike responses of an AON neuron to ipsi-OE (B, black dots and bars) and contra-OE (C, gray dots and bars) odorant stimulation.

A, A single respiration cycle is shown. The spike responses to ipsi-OE and contra-OE stimulation peaked at the inspiration-expiration transition (black histogram) and the expiration phase (gray histogram), respectively. The response to ipsi-OE stimulation was greater than that to contra-OE stimulation.

Fig. 7. Peak of respiration phase-locked spike responses induced *via* the ipsi-pathway precedes that induced *via* the contra-pathway.

A, Comparison of peak latency of respiration phase-locked spike responses induced by contra-nasal odor stimulation (Y axis, one respiration cycle) with that induced by ipsi-nasal odor stimulation (X-axis, one respiration cycle). Each dot represents an individual AON neuron. The averaged peak latency of the spike responses to contra-nasal odor stimulation was significantly longer than that of the spike responses to ipsi-nasal odor stimulation (n=8 cells, wilcoxon t-test, $p < 0.05$).

B, The averaged peak latency of the resumed respiration phase-locked discharges after ipsi-nostril obstruction (Y-axis, one respiration cycle) was significantly longer than that of respiration phase-locked activity before nostril obstruction (X-axis, one respiration cycle) (n=17 cells, wilcoxon t-test, $p < 0.01$).

Fig. 8. Individual AON neurons show nearly equivalent odorant category selectivity for ipsi- and contra-nasal inputs.

A, The odorant category selectivity of each neuron (#1-8) is represented in each row. The filled and open marks indicate significant and absent spike responses to ipsi/contra-OE stimulation with individual odorant categories, respectively. The odorant category selectivity of AON neurons after ipsi- and contra-nasal inputs matched closely, but the latter categories were typically a subset of the former.

B, Odorant selectivity of individual AON neurons does not differ significantly, regardless of whether inputs are from the ipsi- or contra-OE. Small circles with numbers between the upper and lower marks indicate the response to an individual odorant category component. Responses of cell #11 to Ester category are exceptional (one case among 130 different responses listed here) in that the responses are contra-nasal selective. The odorant category marks without small circled numbers indicate that we did not determine the response to individual component odorants of the category. Filled circles, significant response; open circles, no response.

C, X-axis shows the number of odorant category matched (0-10) responses of individual binasal neurons to ipsi-nasal and contra-nasal stimulation, when each

of the ten odorant categories was introduced to the ipsi- and contra-nostrils. Blue columns show the percentage of AON neurons (n=13 cells) with different numbers of odorant category matches. The averaged number of odorant category matches was about 8.2. The grey bars indicate a hypothetical histogram of binominal distribution of neurons with different numbers of odorant category matches, under the assumption of random matching.

Fig. 9. The averaged magnitude of responses to ipsi-nasal odor stimulation exceeds that for contra-nasal odor stimulation.

Each closed circle indicates the averaged magnitude of ipsi-OE- (left) and contra-OE-induced (right) responses in an individual binasal neuron. Open circles indicate the averaged response magnitude among 31 ipsi-OE-induced responses (left, mean±SD, 7.8±1.1) or contra-OE-induced responses (right, 4.7±0.8) (31 binasal neurons, paired t-test, $p<0.01$).

Fig. 10. Binasal mixture facilitation of AON neurons.

A, B, C, Spike activity of a binasal AON neuron induced by ipsi-nasal (A), contra-nasal (C) and bilateral-nasal stimulation (B) with ester category. Shown are

raster representation and peristimulus time histogram of the AON neuron. This neuron showed weak excitatory spike responses to ipsi- and contra-nasal stimulation with ester (***A, C***). When bilaterally stimulated with ester category, this neuron showed robust excitatory responses (***B***).

D, E, F, Spike activity of the same AON neuron induced by ipsi-nasal (D), contra-nasal (F) and bilateral-nasal stimulation (E) with acid category. This neuron showed robust excitatory responses when bilaterally stimulated with acid category, whereas ipsi-nasal only stimulation induced a weak response and contra-nasal stimulation caused no response. F.R.; firing rates. The bar under the histograms indicates the period of odor stimulation (3 s).

Fig. 11. Ipsi-nasal E-0 type AON neurons were preferentially located in layer Ⅱa, while binasal E-E type AON neurons tended to be located in layer Ⅱb.

A, A representative Nissl stained coronal section in the AON. AON are divided into three layers (layer Ⅰ, layer Ⅱ and layer Ⅲ).

B, The laminar distribution of the recorded AON neurons (binasal E-E type and ipsi-nasal E-0 type AON neurons). Most of the recorded AON neurons (37 cells out of 44) were located in the layer Ⅱ.

C, A representative coronal section showing the sublayer specific distribution of binasal E-E type and ipsi-nasal E-0 type AON neurons. Shown are a Nissl stained coronal section with superimposed positions of AON neurons (blue dots; neurons recorded in layer Ⅱa, red dots; neurons recorded in layer Ⅱb). Encircled area in broken black line corresponds to layer Ⅱ. Yellow broken line shows a border of layer Ⅱa and layer Ⅱb. The numbers and alphabets at each dot indicate #cell number, (#rat number), cell type (binasal E-E or ipsi-nasal E-0), respectively.

D, The sublayer specific distribution of binasal E-E type and ipsi-nasal E-0 type AON neurons in Layer Ⅱ. The upper and lower bar indicate the population of the ipsi-nasal E-0 type AON neurons and the binasal E-E type AON neurons in layer Ⅱa and Ⅱb, respectively (red bar; number of the ipsi-nasal E-0 type AON neurons, blue bar; number of the binasal E-E type AON neurons). The ipsi-nasal E-0 type AON neurons were preferentially located in layer Ⅱa. The binasal E-E type AON neurons tended to be located in layer Ⅱb (Fisher's exact probability test, probability of the sublayer specific distribution in the 26 binasal E-E type AON neurons and 11 ipsi-nasal E-0 type AON neurons, $p<0.05$).

Fig. 12. Ipsi-nostril obstruction rapidly enhances individual AON neuron responsiveness to contra-nasal inputs.

A, Time course of the response magnitude (R.M.) of an AON neuron to ipsi-OE (red diamond) or contra-OE (blue square) odorant stimulation (upper trace). Shown are firing rates (F.R.) (1 bin = 0.3 sec, middle) and spike activity (bottom) at times a, b, c and d. This neuron responded only to ipsi-OE stimulation prior to ipsi-nostril obstruction (a and b), but a few minutes following ipsi-nostril obstruction (c and d) it started responding strongly to contra-OE stimulation. Filled triangle, the start of ipsi-nostril obstruction; open triangle, the time of re-opening the ipsi-nostril.

B, Nasal obstruction enhances responsiveness to contra-nasal inputs of AON neurons. Each row (cells 1-3) indicates a raster representation of the spike discharges of an individual AON neuron during inhalation of room air, aligned with the respiratory phase. Spike responses to room air inhalation during one respiration cycle are shown on the Y axis (from the start of inspiration (In.) to the end of expiration (Ex.)). Responses to successive inhalations are arranged on the X axis. After ipsi-nostril obstruction (at time 0, filled triangle), the respiration phase-locked discharges of all three neurons (which peaked at the

inspiration-expiration transition) disappeared, but then reappeared about 300 sec later (filled diamond) with a peak at the expiration phase. Open triangle, the time of re-opening the ipsi-nostril.

Fig. 13. Enhancement of contra-nasal input is triggered by the ipsi-nostril obstruction.

Shown are time course of the response magnitude (R.M.) of an AON neuron to ipsi-OE (red diamond) or contra-OE (blue square) odorant stimulation. This neuron responded strongly to ipsi-OE stimulation (a) and slightly to contra-OE stimulation (b) with terpene hydrocarbon category. The repeated contra-OE stimulation without ipsi-nostril obstruction does not induce the heightened responsiveness to contra-OE stimulation during about 300 sec. After ipsi-nostril obstruction, this cell started responding strongly to contra-OE stimulation about a minute later (c)

Fig. 14. Enhancement of contra-nasal input occurs independently of the increase in contra-nasal airflow.

A, Time course of the magnitude of responses (M.R.) to ipsi-OE (red diamond) or

contra-OE (blue square) stimulation (upper trace). Spike discharges and their histograms (1 bin = 0.3 sec) showing responses to odor stimulation at time points a, b, c and d are shown in the middle trace. The bottom trace in each column indicates nasal airflow at the contra-nostril. The cell shown responded strongly to ipsi-OE stimulation with the phenol category (a) and relatively weakly to contra-OE stimulation with the phenol category (b). About 100 sec following ipsi-nostril obstruction, the cell responded to contra-OE stimulation (c) much more strongly. No systematic change in airflow was observed at this time point.

B, Simultaneous recordings from an AON neuron of spike discharges (upper), airflow rate (middle) and nasal airflow at the contra-nostril (lower). Upper row indicates raster representation of the spike discharges of an AON neuron aligned with the respiratory phase (from the start of inspiration (In.) to the end of expiration (Ex.)). In the absence of odor stimulation, the cell showed spike discharges that were phase-locked to the inhalation of the room air. After ipsi-nostril obstruction (at time 0, filled triangle), the nasal airflow clearly increased (a) and then remained relatively stable, even during the period when the respiration phase-locked discharges reappeared about 100 sec later (b, filled diamond). Open triangle indicates the time when obstruction was removed (c).

Fig. 15. A schematic diagram illustrating co-ordinated neuronal connections between ipsi-lateral and contra-lateral AONs.

Possible neuronal circuits mediating the bilateral matching of odorant selectivity for right and left nasal inputs. Individual binasal AON neurons were tuned to specific combinations of odorant categories. The odorant category selectivity for ipsi-nasal inputs closely resembles that for contra-nasal inputs.

Fig. 16. The morphology of a binasal E-E type neuron.

A, Shown are a raster representation of the spike responses and peristimulus time histograms. This cell showed excitatory responses to both ipsi-nasal and contra-nasal stimulation with ether category, thus identified as binasal E-E type AON neuron. Colored bar; duration of odor stimulation (ether category, 3 sec).

B, Morphology of the binasal E-E type AON neuron labeled with 4% biotinylated dextran amine by juxtacellular iontophoresis (pulse intensity; <10 μ A, injection time; 20 min, survival period; 6 hr). This cell was located in the border between layer Ⅱa and Ⅱb.

C, Higher signification reveals basal dendrites (double arrow head) extending from soma and apical dendrites (arrow head) reaching out toward superficial part

of the layer Ⅰ. Some fine branches of the axonal arbolization are visible (arrow).

Fig. 1

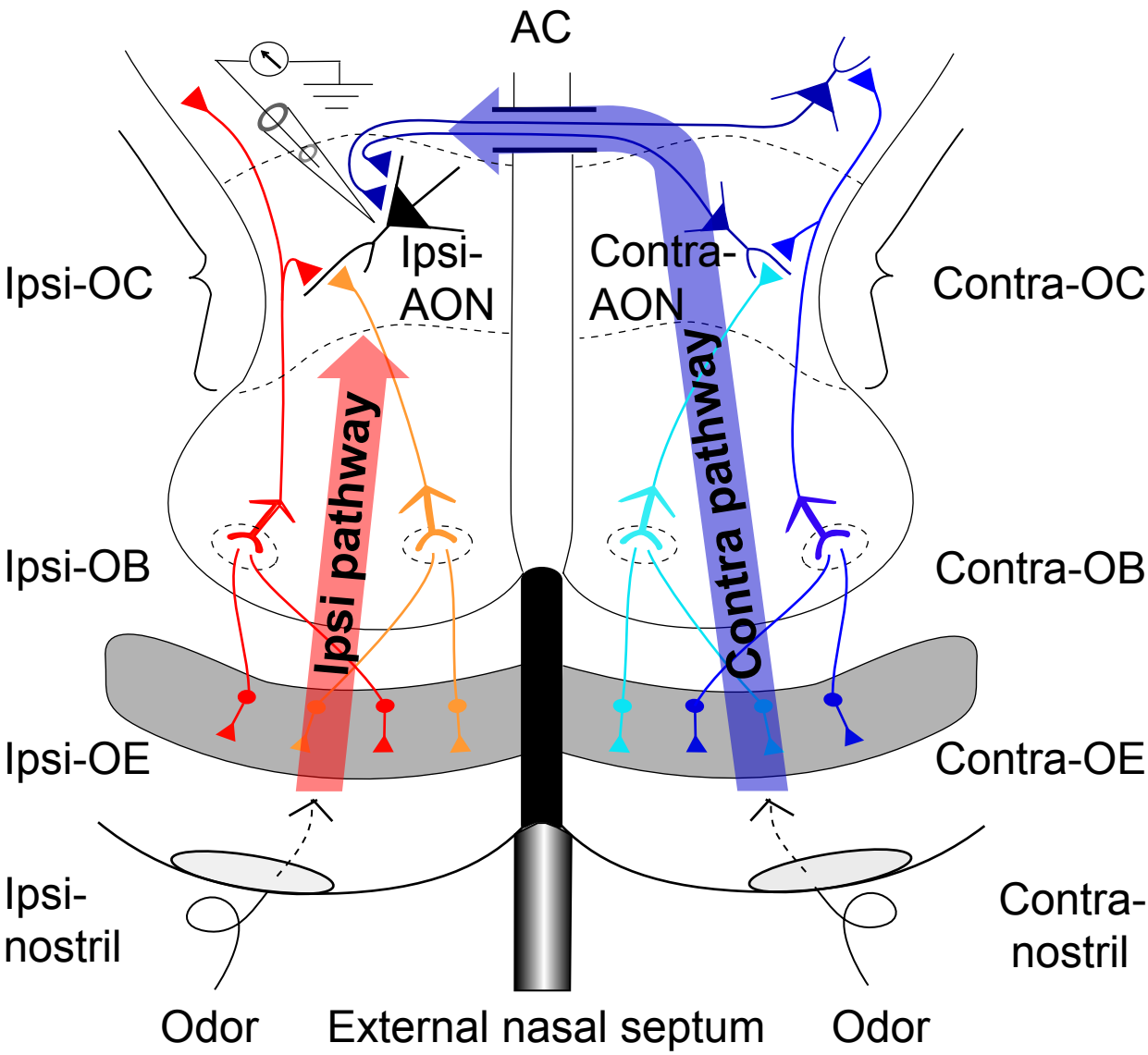
AC
Ipsi-OC
Ipsi-AON
Contra-AON
Contra-OC
Ipsi pathway
Contra pathway
Ipsi-OB
Contra-OB
Ipsi-OE
Contra-OE
Ipsi-nostril
Contra-nostril
Odor
External nasal septum
Odor

Fig. 2

A. Sulfide category				
① 1-hexanethiol (6-SH) 	② 1-octanethiol (8-SH)	③ propyl sulfide 	④ ethyl sulfide 	⑤ tetrahydrothiophene 
B. Ester category				
① ethyl butyrate 	② amyl hexanoate 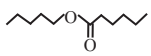	③ b-γ-hexenyl acetate 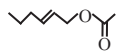	④ terpinyl acetate 	⑤ isoamyl acetate 
C. Terpene hydrocarbon category				
① myrcene 	② d-limonene 	③ α-pinene 	④ α-phellandrene 	⑤ α-cadinene 
D. Acid category				
① propionic acid 	② n-hexanoic acid 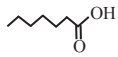	③ n-Nonanoic acid 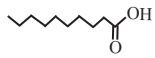	④ cyclopentane carboxylic acid 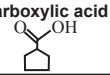	⑤ n-methyl butyric acid 
E. Ether category				
① methyl n-propyl ether 	② dipropyl ether 	③ butyl methyl ether 	④ hexyl metyl ether 	⑤ butyl ethyl ether 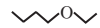
F. Aldehyde category				
① propylaldehyde 	② n-valeraldehyde 	③ n-heptylaldehyde 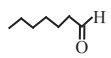	④ benzaldehyde 	⑤ perilla aldehyde 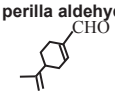
G. Lactone category				
① γ-butyrolactone 	② γ-heptalactone 	③ δ-hexalactone 	④ δ-nonalactone 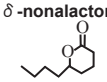	⑤ γ-octalactone 
H. Alcohol category				
① propylalcohol 	② n-hexyl alcohol 	③ n-octyl alcohol	④ cis-3-hexenol 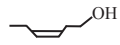	⑤ benzyl alcohol 
I. Ketone category				
① n-propyl methyl ketone	② n-heptyl ethyl ketone	③ carvone	④ amyl cyclopentanone	⑤ 3-methyl-2-cyclopentenone
J. Phenol category				
① eugenol	② anisol	③ o-ethyl phenol	④ p-n-propyl phenol	⑤ 4-ethyl guaiacol

Fig. 3

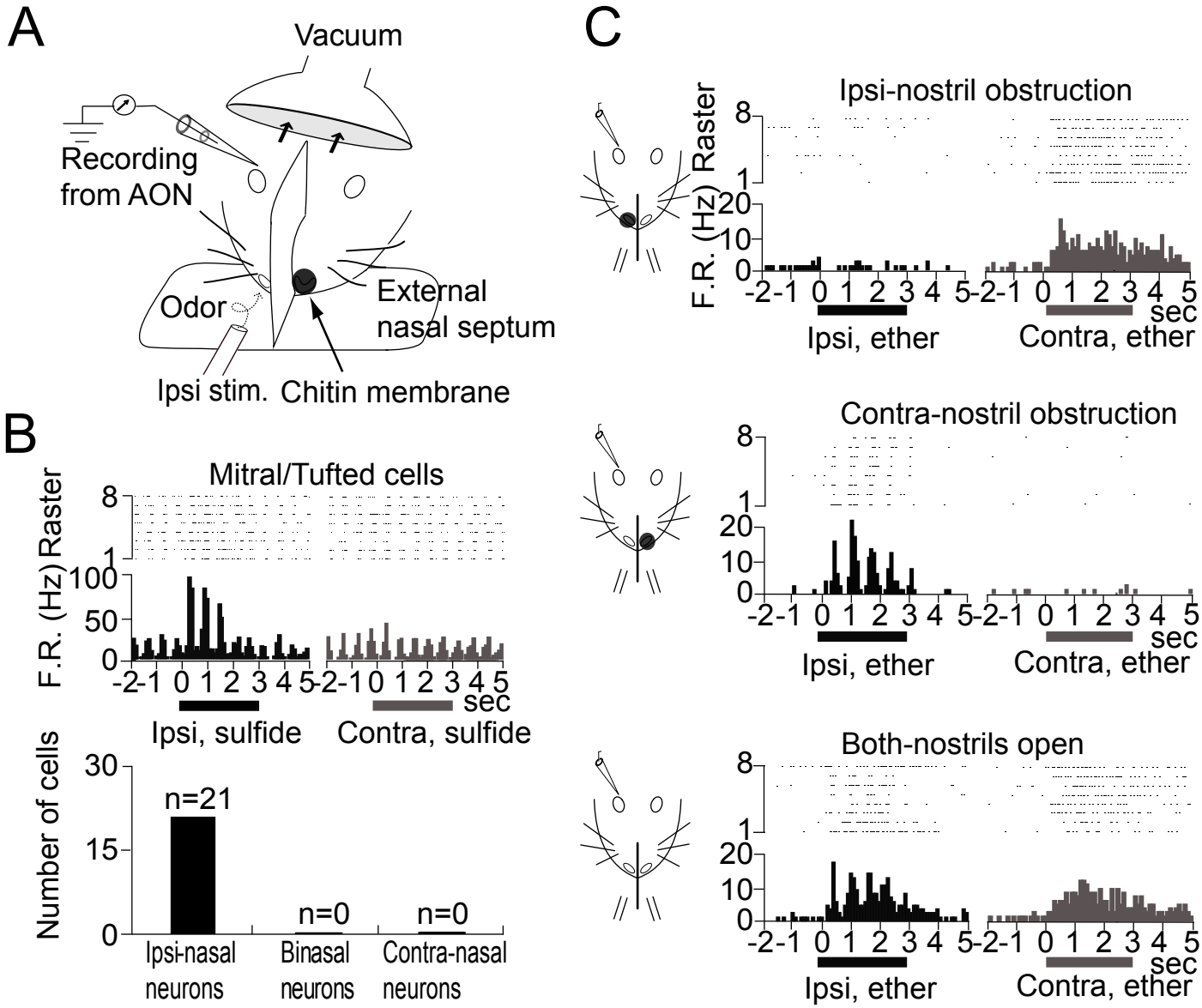
A
Vacuum
Recording
from AON
Odor
External
nasal septum
Ipsi stim.
Chitin membrane
B
Mitral/Tufted cells
F.R. (Hz)
Raster
sec
Ipsi, sulfide
Contra, sulfide
Number of cells
n=21
n=0
n=0
Ipsi-nasal
neurons
Binasal
neurons
Contra-nasal
neurons
C
Ipsi-nostril obstruction
Ipsi, ether
Contra, ether
Contra-nostril obstruction
Ipsi, ether
Contra, ether
Both-nostrils open
Ipsi, ether
Contra, ether

Fig. 4

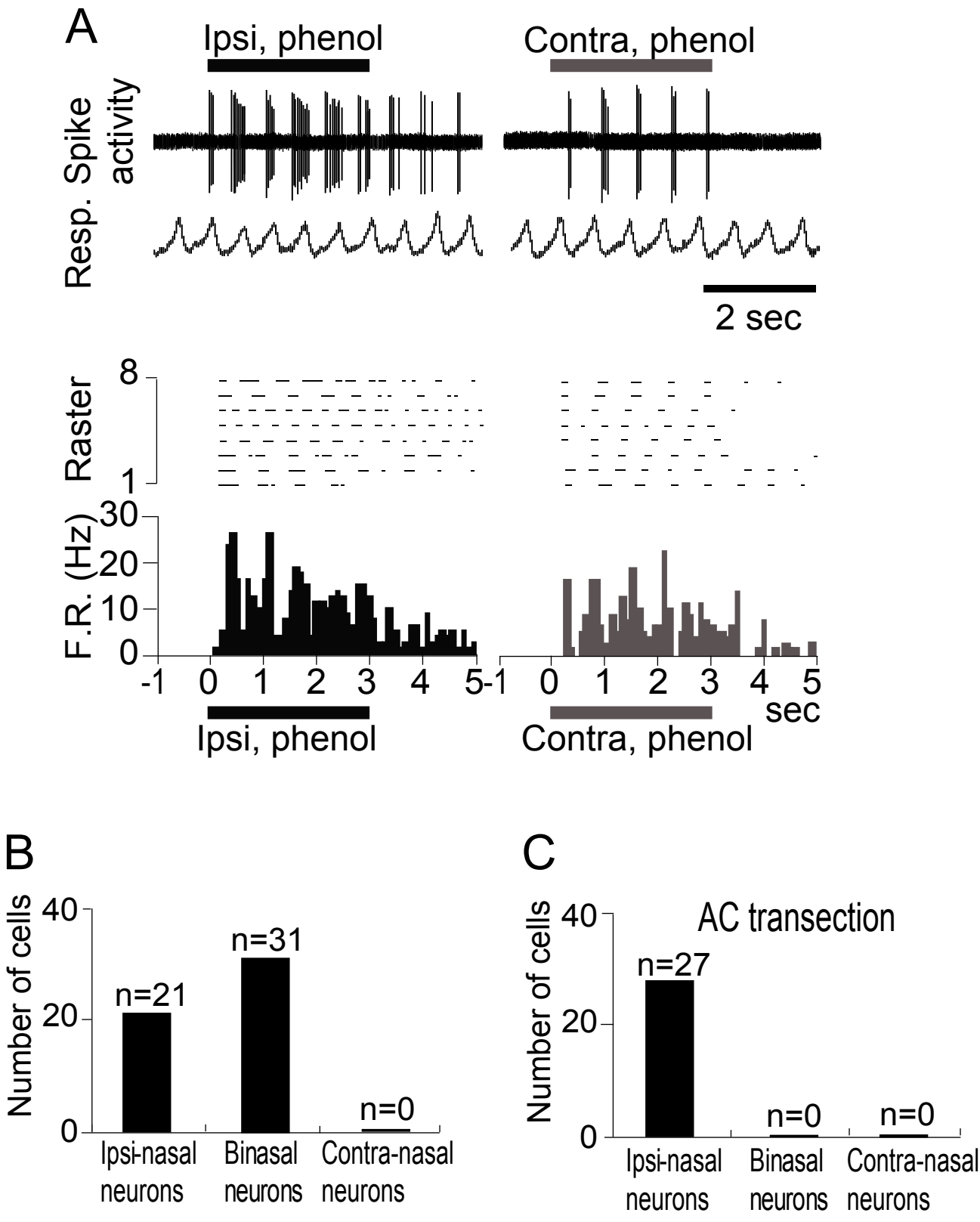
A
Ipsi, phenol
Contra, phenol
Resp. Spike activity
2 sec
Raster
8
1
F.R. (Hz)
30
20
10
0
-1 0 1 2 3 4 5
-1 0 1 2 3 4 5
sec
Ipsi, phenol
Contra, phenol
B
Number of cells
40
20
0
n=21
n=31
n=0
Ipsi-nasal neurons
Binasal neurons
Contra-nasal neurons
C
AC transection
Number of cells
40
20
0
n=27
n=0
n=0
Ipsi-nasal neurons
Binasal neurons
Contra-nasal neurons

Fig. 5

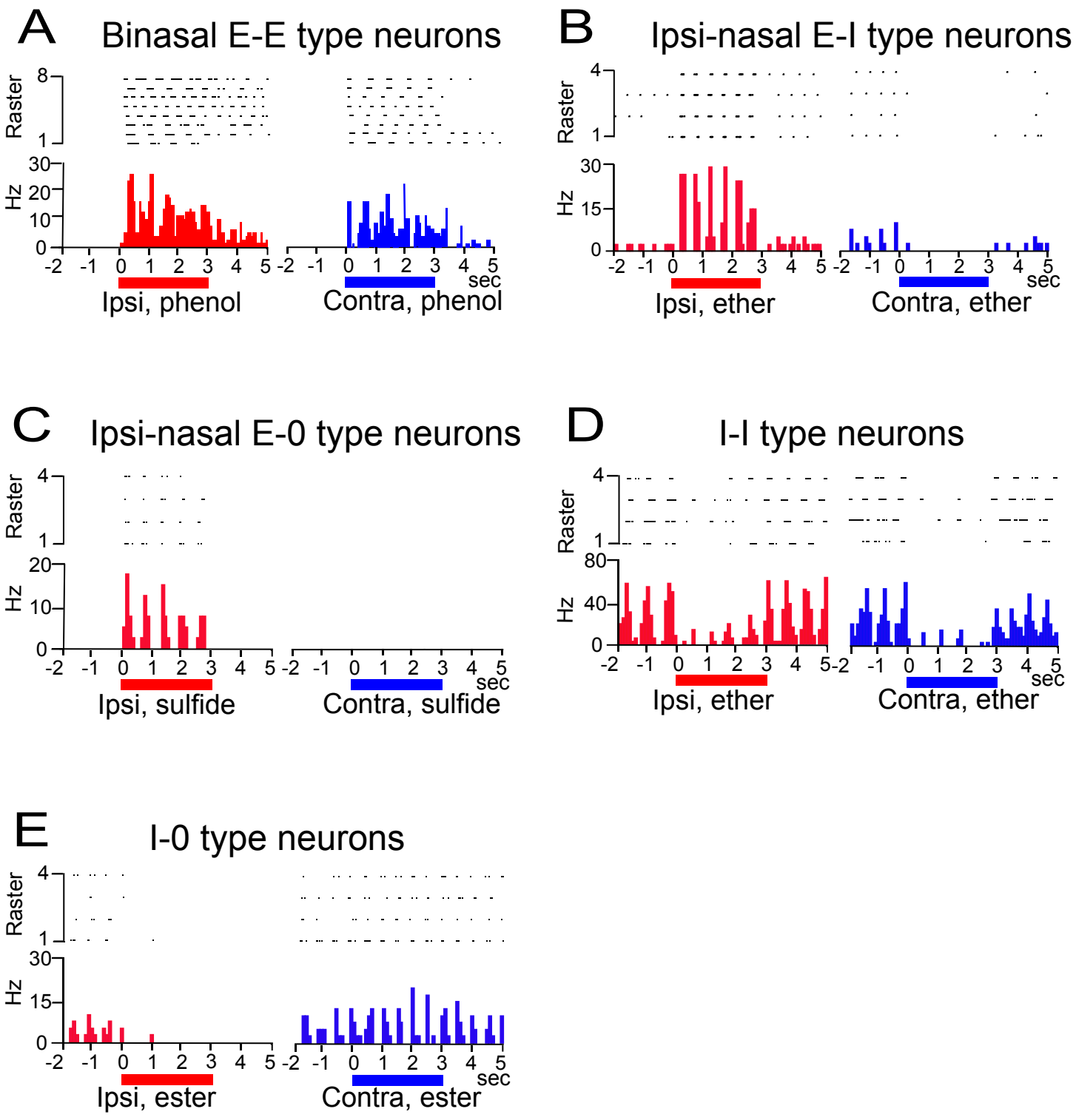
A
Binasal E-E type neurons
Raster
Hz
Ipsi, phenol
Contra, phenol
B
Ipsi-nasal E-I type neurons
Raster
Hz
Ipsi, ether
Contra, ether
C
Ipsi-nasal E-0 type neurons
Raster
Hz
Ipsi, sulfide
Contra, sulfide
D
I-I type neurons
Raster
Hz
Ipsi, ether
Contra, ether
E
I-0 type neurons
Raster
Hz
Ipsi, ester
Contra, ester
sec

Fig. 6

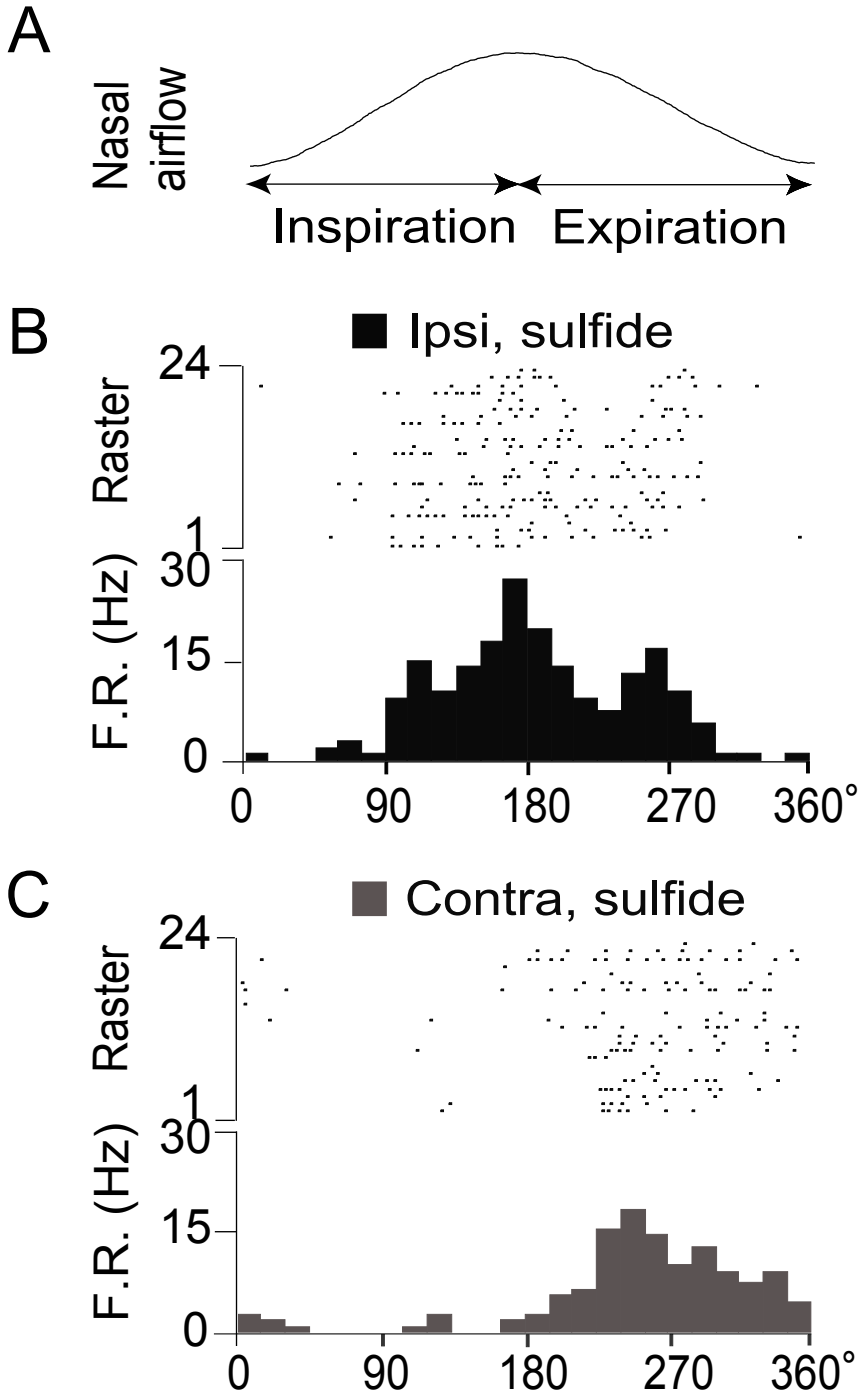
A
Nasal airflow
Inspiration
Expiration
B
Ipsi, sulfide
Raster
24
1
F.R. (Hz)
30
15
0
0
90
180
270
360°
C
Contra, sulfide
Raster
24
1
F.R. (Hz)
30
15
0
0
90
180
270
360°

Fig. 7

A

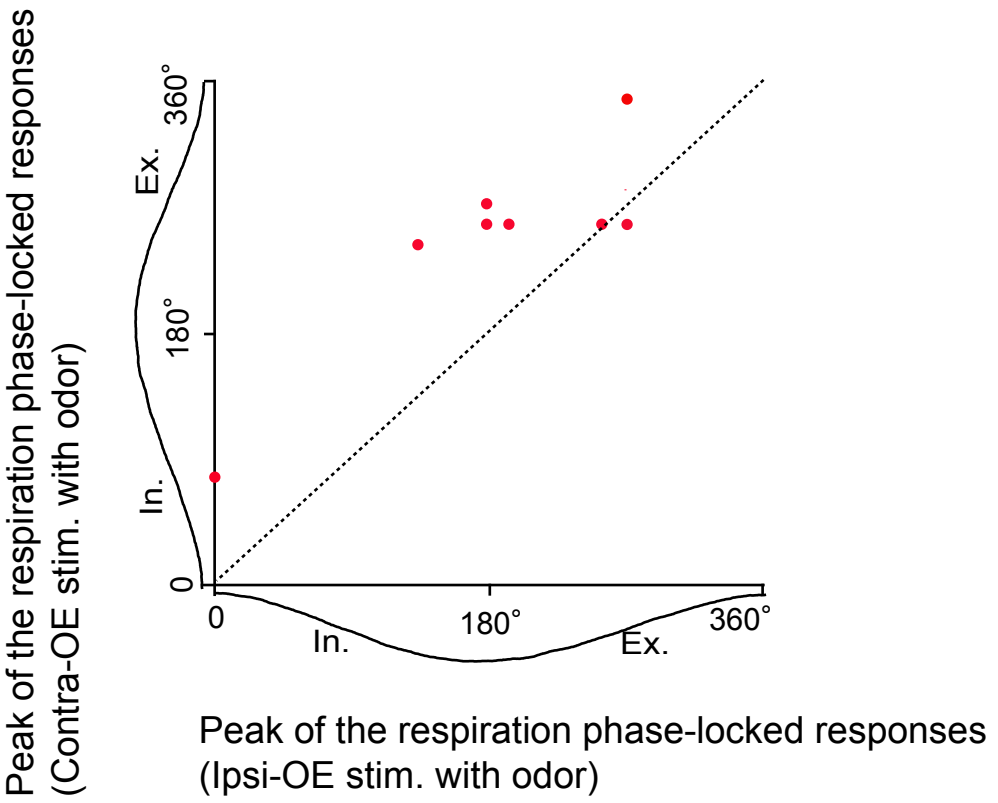
Peak of the respiration phase-locked responses
(Contra-OE stim. with odor)
Ex.
360°
180°
In.
0
0
180°
360°
In.
Ex.
Peak of the respiration phase-locked responses
(Ipsi-OE stim. with odor)

B

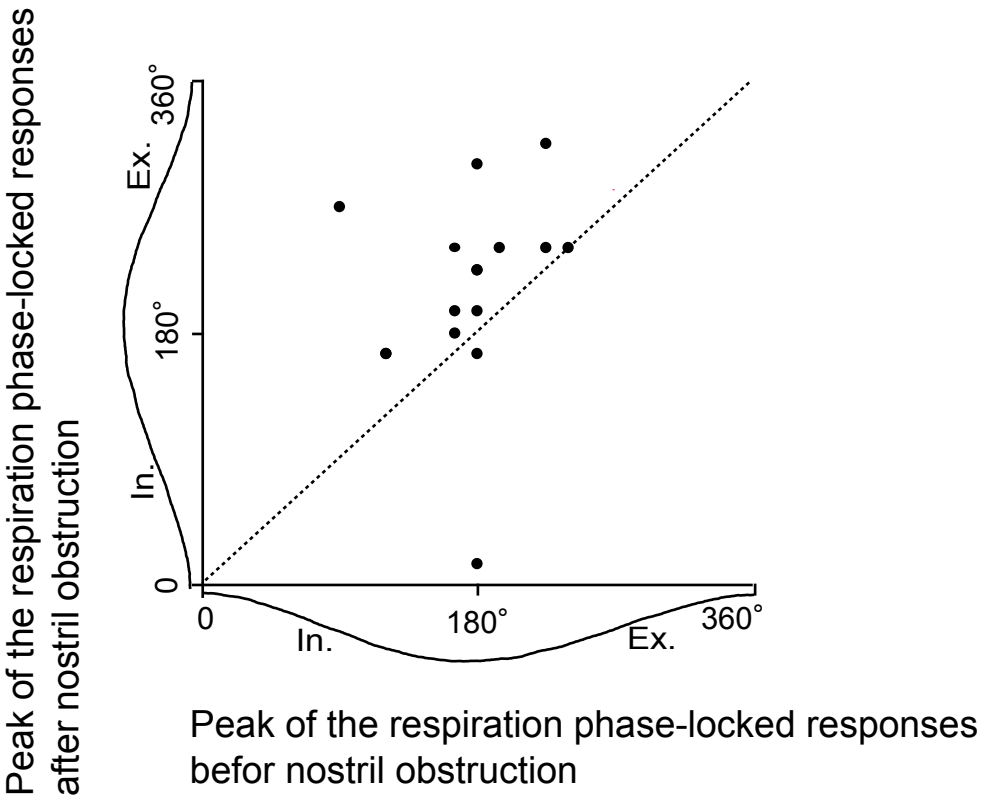
Peak of the respiration phase-locked responses
after nostril obstruction
Ex.
360°
180°
In.
0
0
180°
360°
In.
Ex.
Peak of the respiration phase-locked responses
befor nostril obstruction

Fig. 8

A

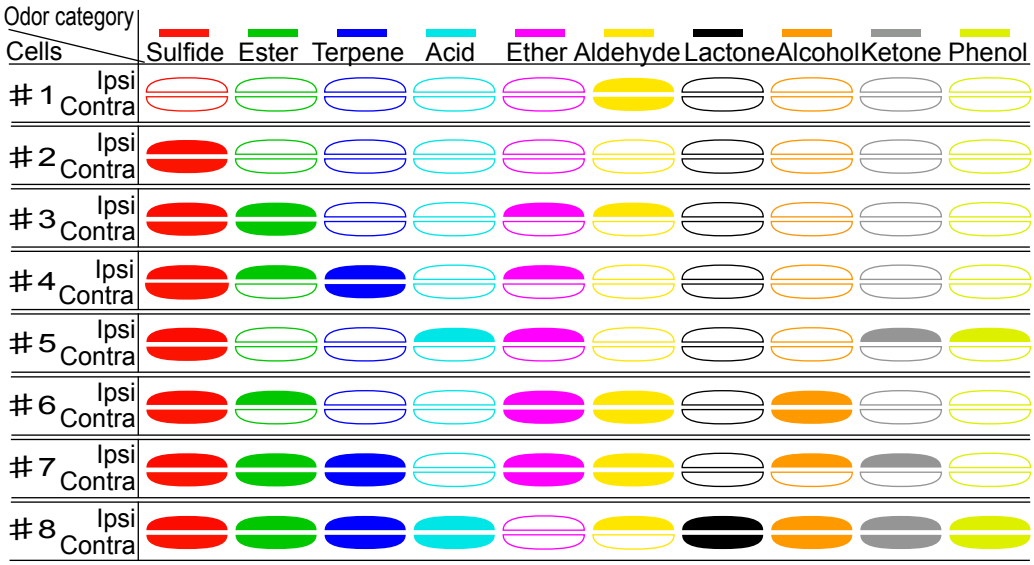
Odor category
Cells
Sulfide
Ester
Terpene
Acid
Ether
Aldehyde
Lactone
Alcohol
Ketone
Phenol
#1
#2
#3
#4
#5
#6
#7
#8
Ipsi
Contra

B

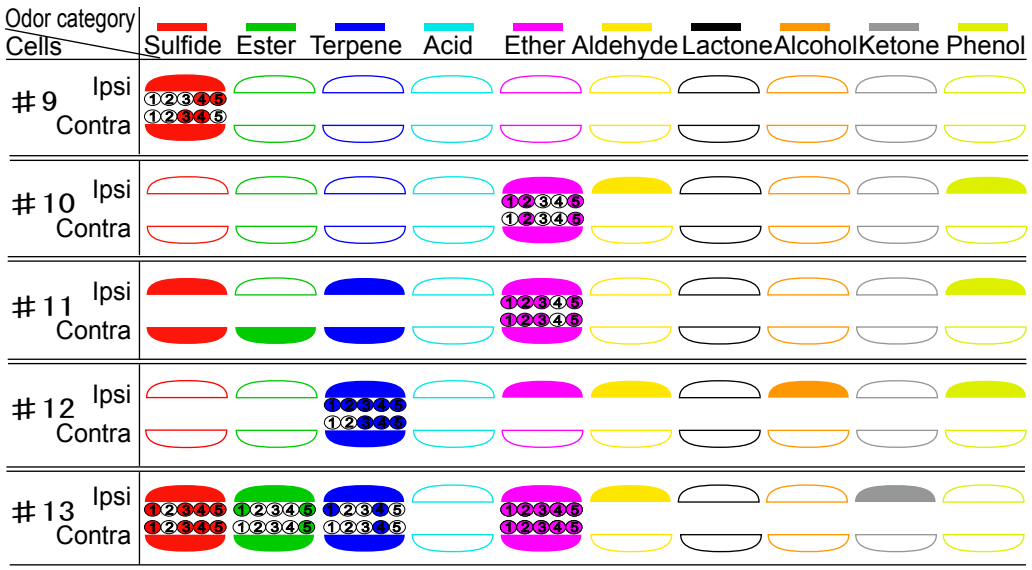
Odor category
Cells
Sulfide
Ester
Terpene
Acid
Ether
Aldehyde
Lactone
Alcohol
Ketone
Phenol
#9
#10
#11
#12
#13
Ipsi
Contra

C

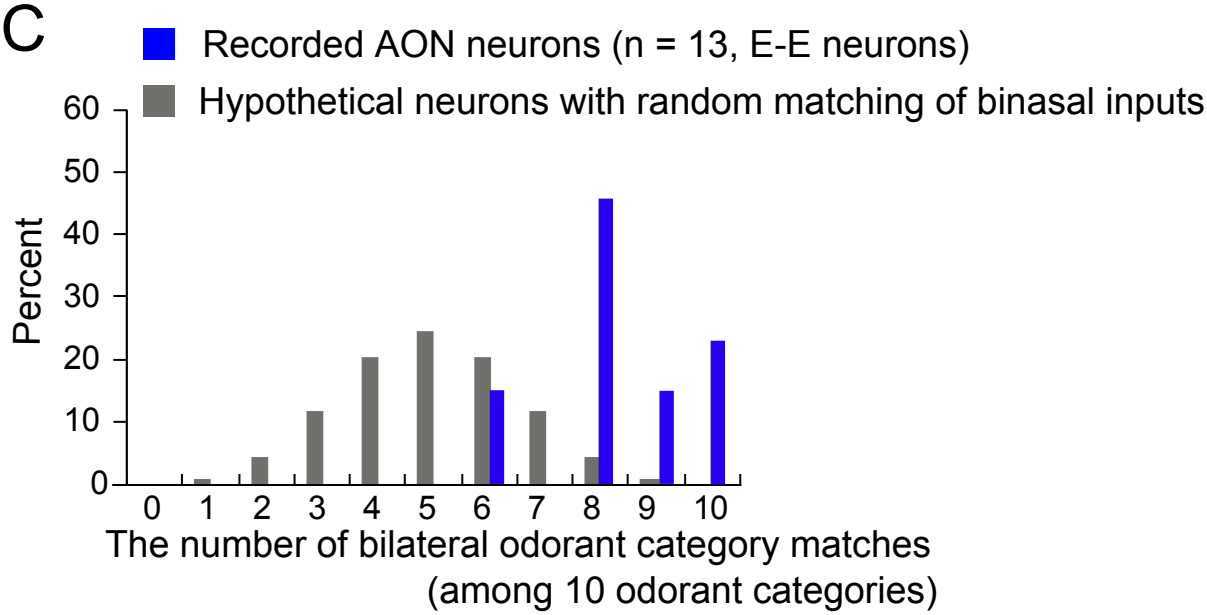
Recorded AON neurons (n = 13, E-E neurons)
Hypothetical neurons with random matching of binasal inputs
Percent
0
10
20
30
40
50
60
0
1
2
3
4
5
6
7
8
9
10
The number of bilateral odorant category matches
(among 10 odorant categories)

Fig. 9

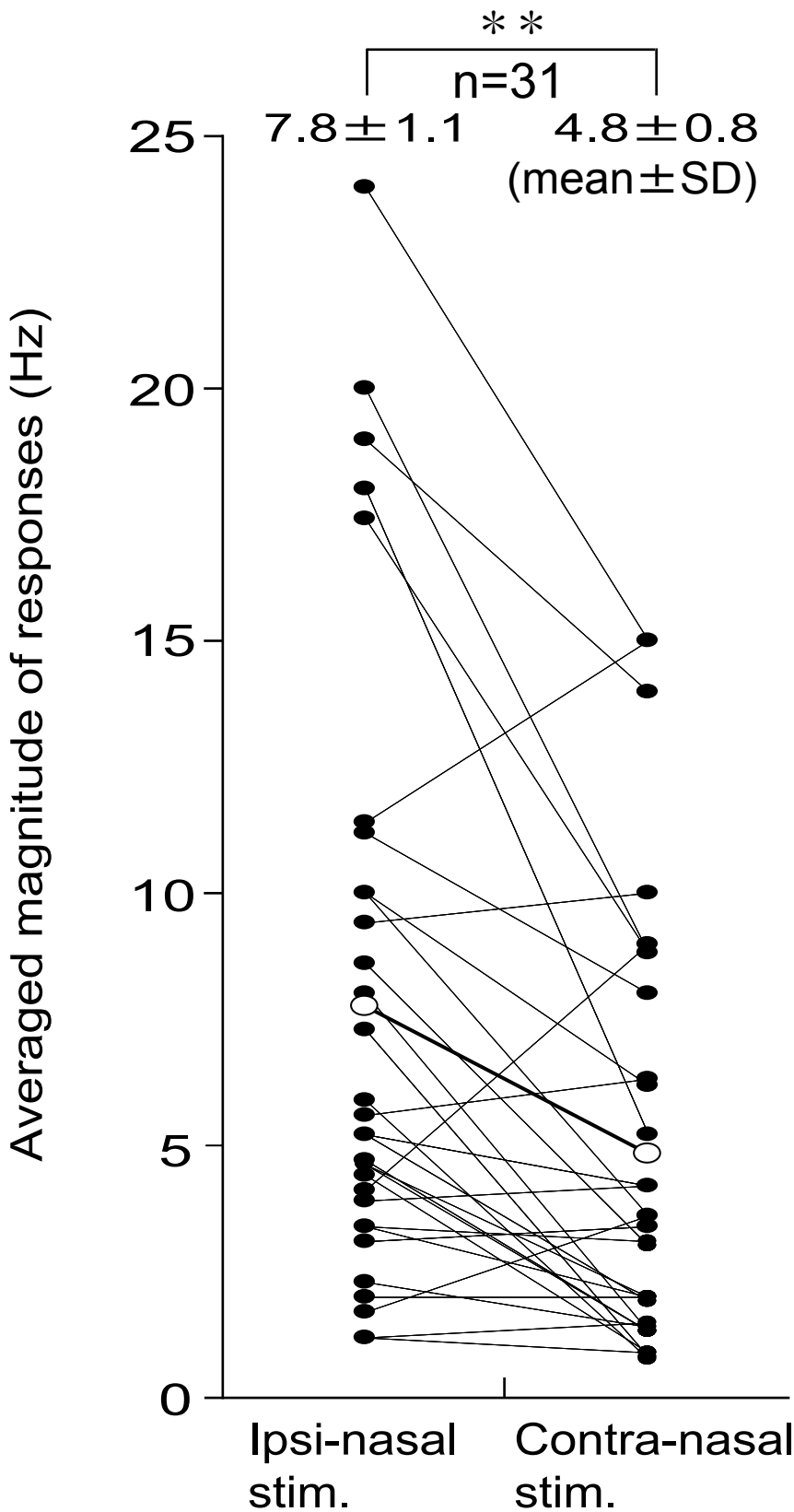
＊＊
n=31
7.8±1.1
4.8±0.8
(mean±SD)
Averaged magnitude of responses (Hz)
25
20
15
10
5
0
Ipsi-nasal stim.
Contra-nasal stim.

Fig. 10

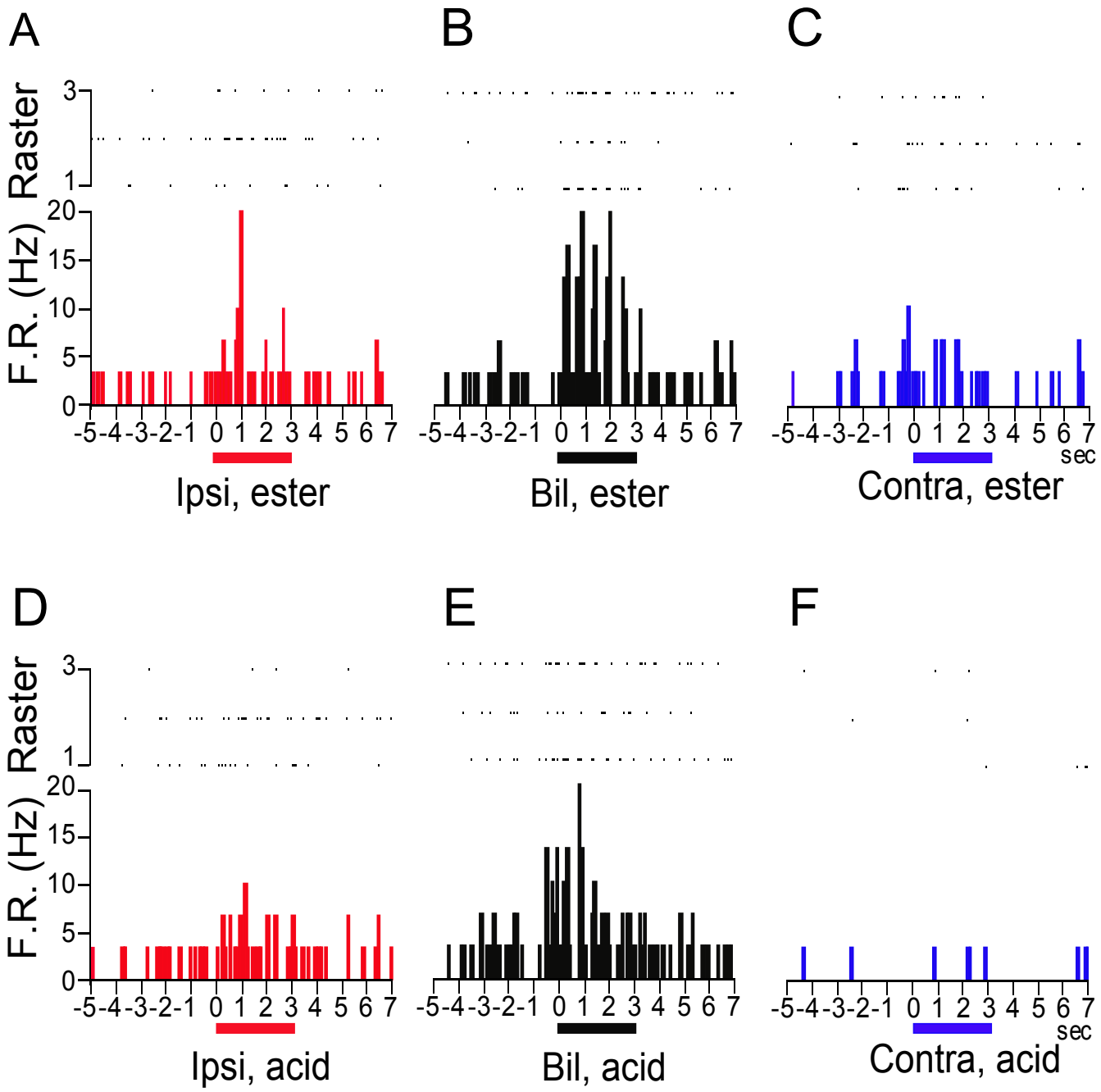
A
B
C
D
E
F
Raster
F.R. (Hz)
3
1
20
15
10
5
0
-5 -4 -3 -2 -1 0 1 2 3 4 5 6 7
sec
Ipsi, ester
Bil, ester
Contra, ester
Ipsi, acid
Bil, acid
Contra, acid

Fig. 11.

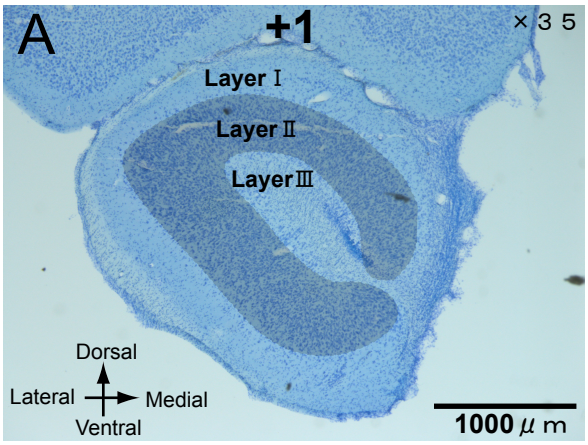
A
+1
× 3 5
Layer Ⅰ
Layer Ⅱ
Layer Ⅲ
Dorsal
Lateral
Medial
Ventral
1000 μ m

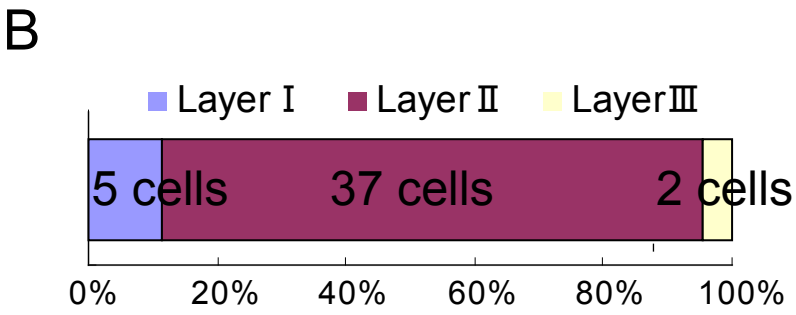
B
Layer Ⅰ
Layer Ⅱ
Layer Ⅲ
5 cells
37 cells
2 cells
0%
20%
40%
60%
80%
100%

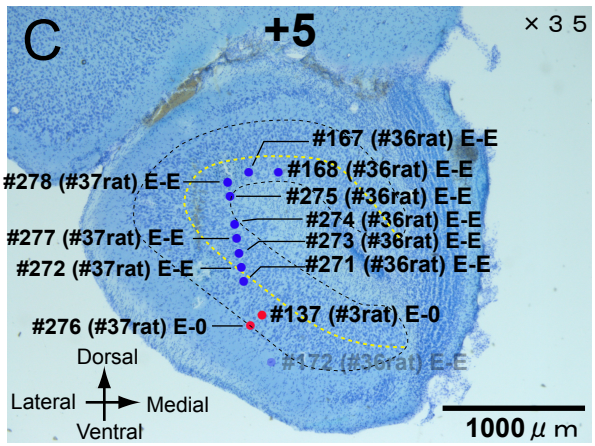
C
+5
× 3 5
#167 (#36rat) E-E
#168 (#36rat) E-E
#278 (#37rat) E-E
#275 (#36rat) E-E
#274 (#36rat) E-E
#277 (#37rat) E-E
#273 (#36rat) E-E
#272 (#37rat) E-E
#271 (#36rat) E-E
#137 (#3rat) E-0
#276 (#37rat) E-0
Dorsal
Lateral
Medial
Ventral
1000 μ m

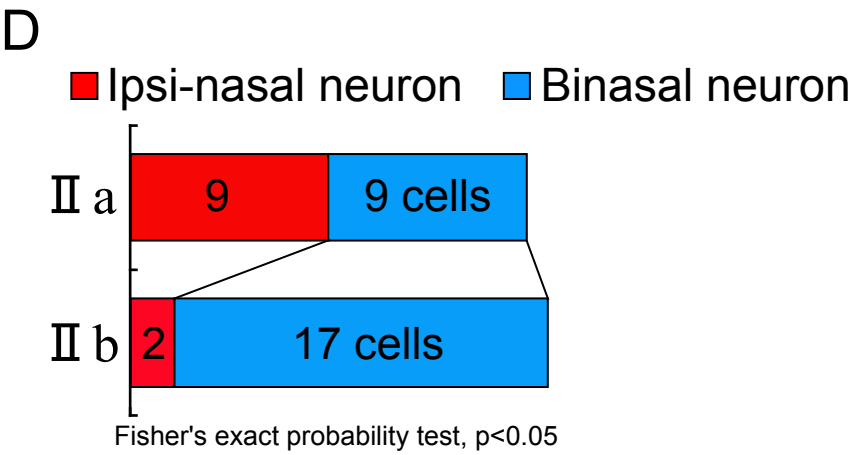
D
Ipsi-nasal neuron
Binasal neuron
Ⅱ a
9
9 cells
Ⅱ b
2
17 cells
Fisher's exact probability test, p<0.05

Fig. 12

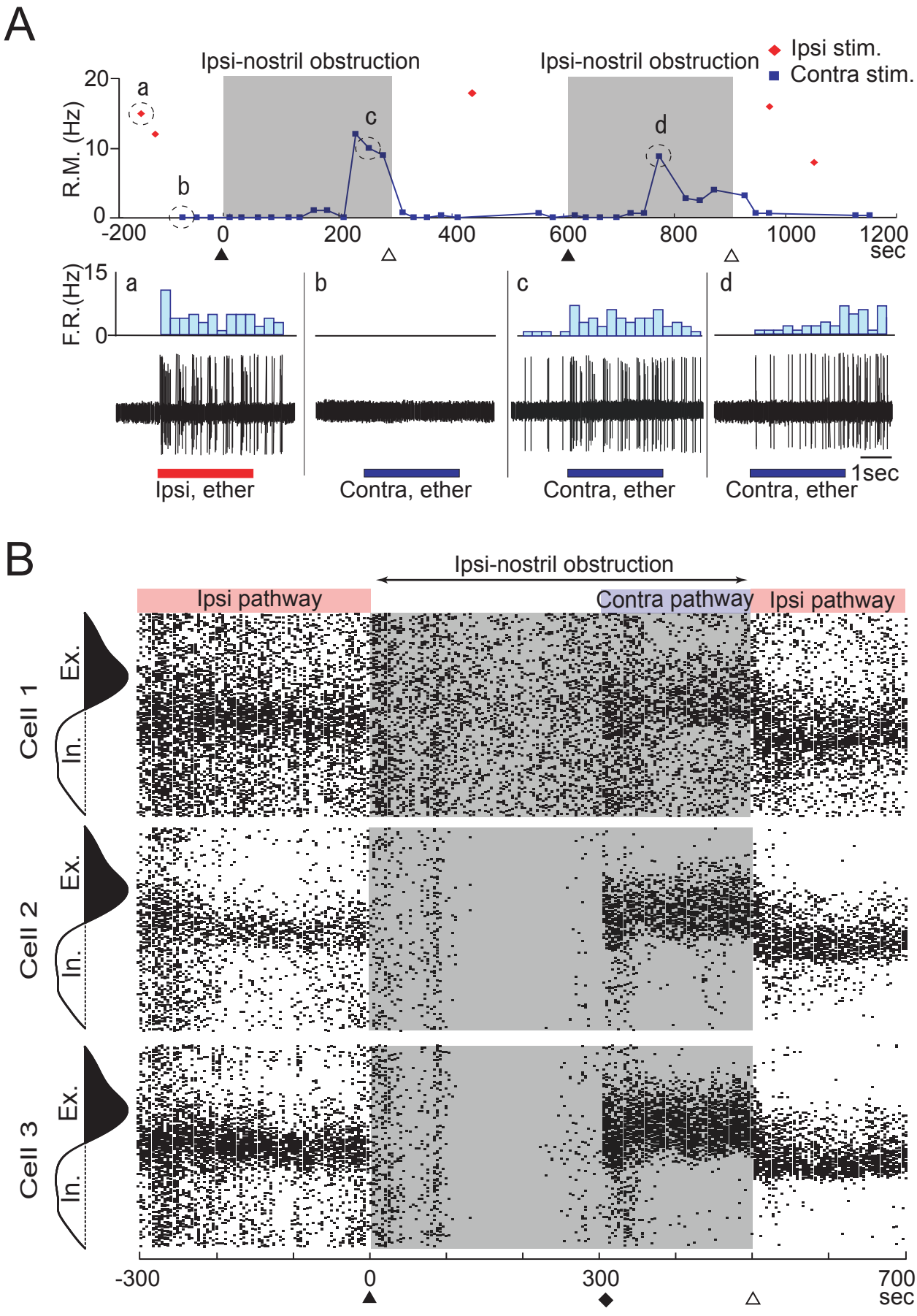
A
Ipsi-nostril obstruction
Ipsi-nostril obstruction
Ipsi stim.
Contra stim.
R.M. (Hz)
20
10
0
a
b
c
d
-200
0
200
400
600
800
1000
1200
sec
F.R.(Hz)
15
0
a
b
c
d
1sec
Ipsi, ether
Contra, ether
Contra, ether
Contra, ether
B
Ipsi-nostril obstruction
Ipsi pathway
Contra pathway
Ipsi pathway
Cell 1
Cell 2
Cell 3
Ex.
In.
-300
0
300
700
sec

Fig. 13

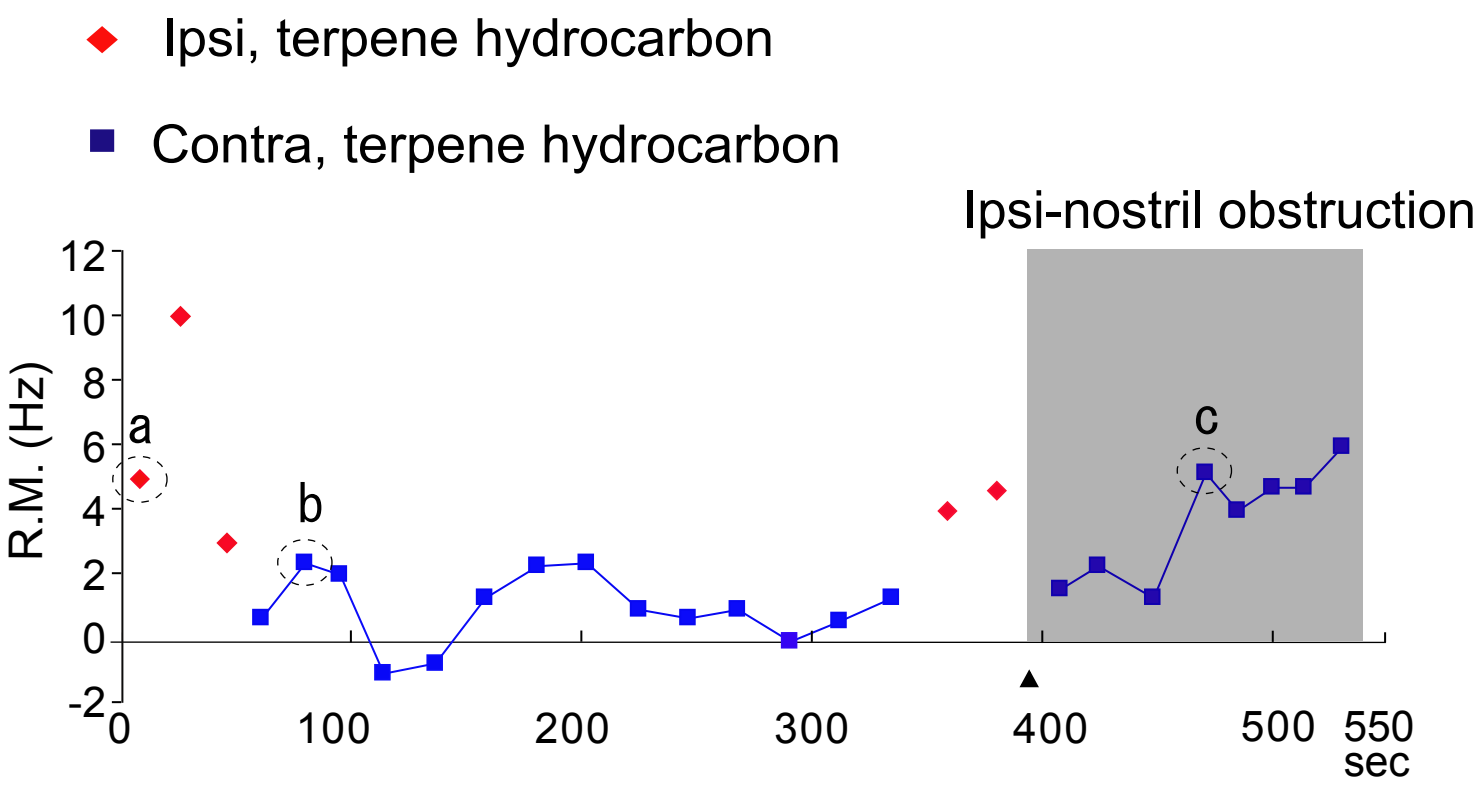
Ipsi, terpene hydrocarbon
Contra, terpene hydrocarbon
Ipsi-nostril obstruction
R.M. (Hz)
12
10
8
6
4
2
0
-2
a
b
c
0
100
200
300
400
500
550
sec

Fig. 14

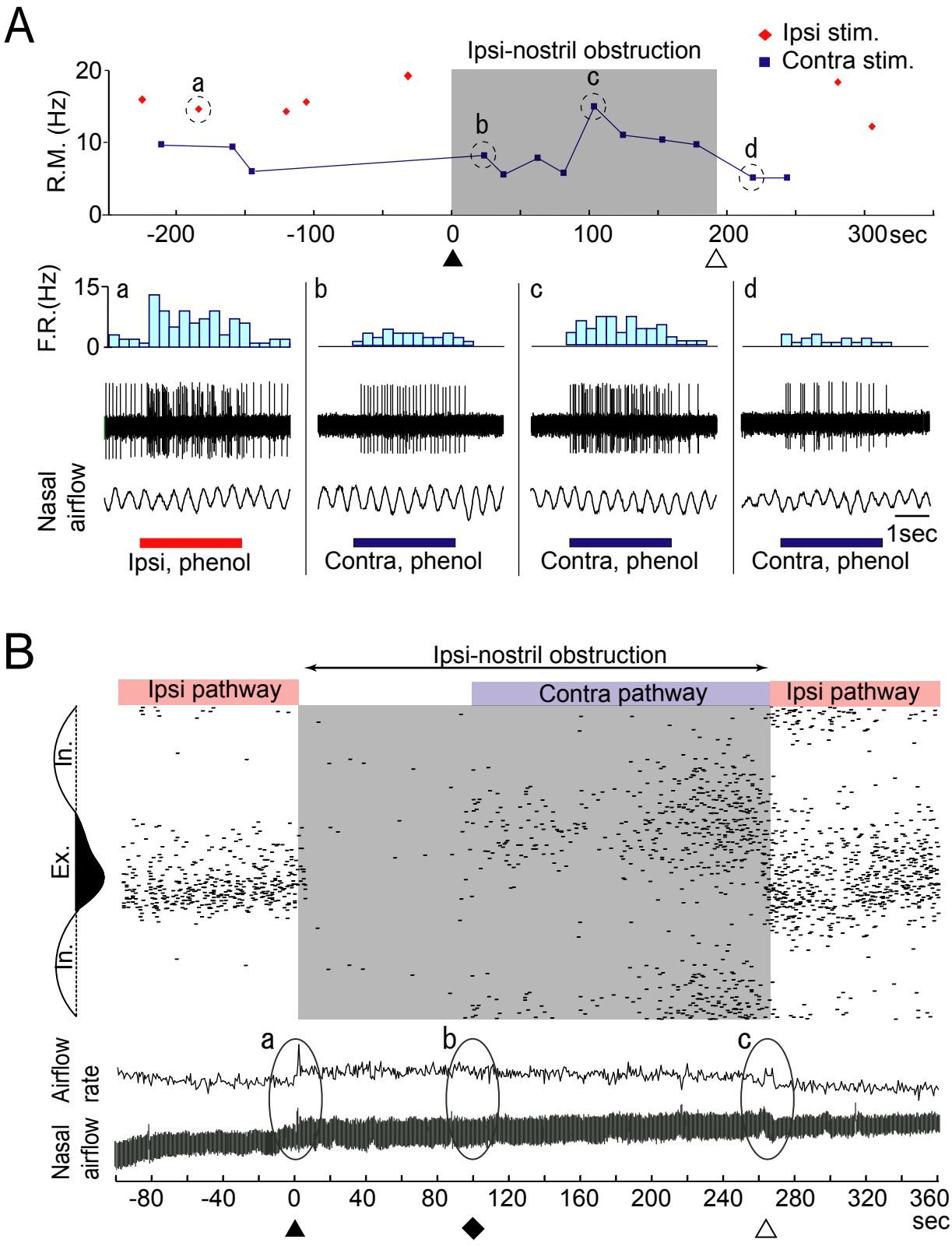
A
Ipsi stim.
Contra stim.
Ipsi-nostril obstruction
R.M. (Hz)
20
10
0
a
b
c
d
-200
-100
0
100
200
300sec
F.R.(Hz)
15
0
Nasal airflow
1sec
Ipsi, phenol
Contra, phenol
Contra, phenol
Contra, phenol
B
Ipsi-nostril obstruction
Ipsi pathway
Contra pathway
Ipsi pathway
In.
Ex.
In.
Airflow rate
Nasal airflow
-80
-40
0
40
80
120
160
200
240
280
320
360
sec

Fig. 15

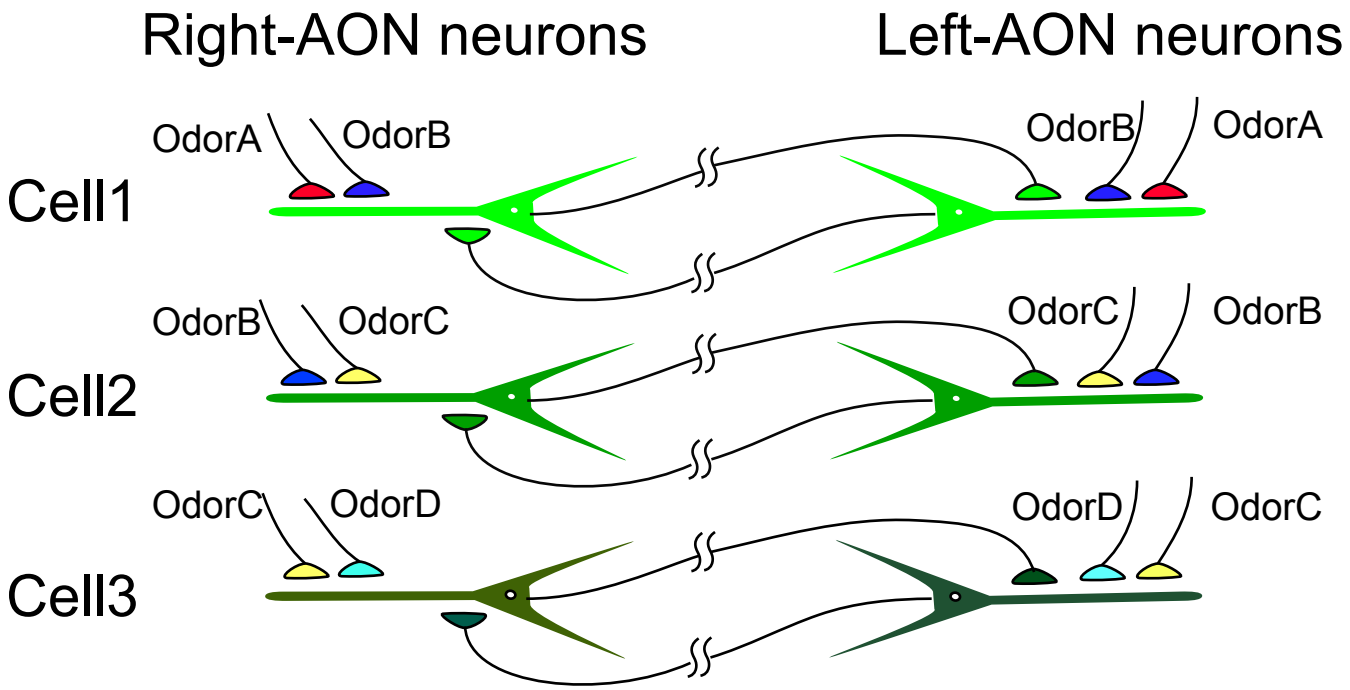
Right-AON neurons
Left-AON neurons
Cell1
OdorA
OdorB
OdorB
OdorA
Cell2
OdorB
OdorC
OdorC
OdorB
Cell3
OdorC
OdorD
OdorD
OdorC

Fig. 16

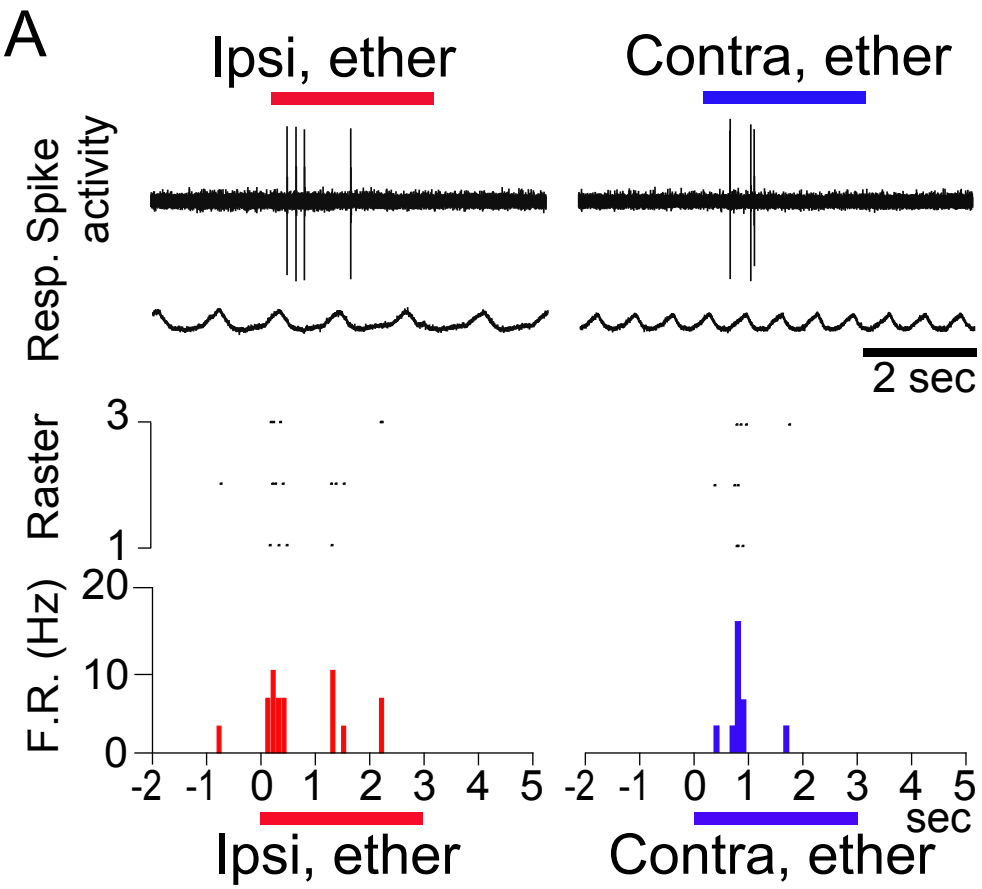
A
Ipsi, ether
Contra, ether
Resp. Spike activity
2 sec
Raster
3
1
F.R. (Hz)
20
10
0
-2 -1 0 1 2 3 4 5
-2 -1 0 1 2 3 4 5
sec
Ipsi, ether
Contra, ether

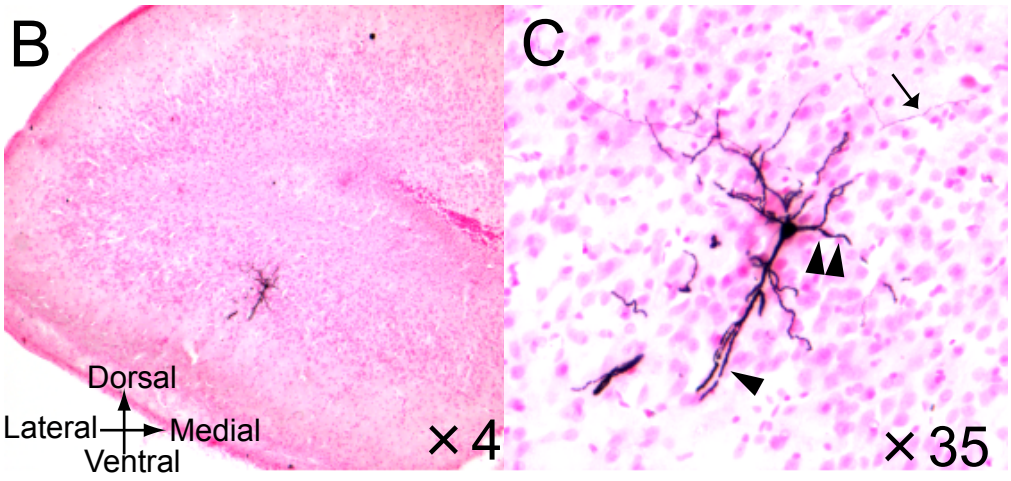
B
Dorsal
Lateral
Medial
Ventral
×4
C
×35

Table 1

Lists of binasal (E-E) and ipsi-nasal (E-0, E-I) neurons in each rat

AON neurons

Rats	Cells	E-E, E-0 type	Ipsi. v.s. Contra ※1	Boost-up ※2	Matching number (0-10) ※3
#1	1	Binasal (E-E)	[I] > [C]	n.d.	8
	2	Binasal (E-E)	[I] > [C]	n.d.	8
	3	Binasal (E-E)	[I]≒[C]	n.d.	10
#2	1	Binasal (E-E)	[I] < [C]	n.d.	10
	2	Binasal (E-E)	[I]≒[C]	n.d.	10
	3	Ipsi-nasal (E-0)	n.d.	n.d.	n.d.
	4	n.d.	n.d.	Y	n.d.
	5	Binasal (E-E)	[I] > [C]	Y	9
	6	Binasal (E-E)	[I] > [C]	n.d.	6
#3	1	Binasal (E-E)	[I] > [C]	Y	9
	2	Ipsi-nasal (E-0)	n.d.	N	n.d.
#4	1	Binasal (E-E)	[I]≒[C]	N	n.d.
	2	Ipsi-nasal (E-0)	n.d.	n.d.	n.d.
#5	1	Ipsi-nasal (E-0)	n.d.	N	n.d.
	2	Ipsi-nasal (E-0)	n.d.	N	n.d.
	3	Binasal (E-E)	[I] > [C]	Y	8
	4	Binasal (E-E)	[I] < [C]	n.d.	8
#6	1	Ipsi-nasal (E-0)	n.d.	N	n.d.
#7	1	Binasal (E-E)	[I] > [C]	Y	n.d.
	2	Binasal (E-E)	[I]≒[C]	Y	n.d.
#8	1	Binasal (E-E)	[I] > [C]	Y	n.d.
	2	Binasal (E-E)	[I] > [C]	N	n.d.
	3	Binasal (E-E)	[I] > [C]	Y	n.d.
	4	Binasal (E-E)	[I] > [C]	N	n.d.
#9	1	Binasal (E-E)	[I] > [C]	N	n.d.
	2	Ipsi-nasal (E-0)	n.d.	N	n.d.
#10	1	Binasal (E-E)	[I] > [C]	N	n.d.
#11	1	Ipsi-nasal (E-I)	n.d.	n.d.	n.d.
	2	Ipsi-nasal (E-0)	n.d.	N	n.d.
	3	Ipsi-nasal (E-0)	n.d.	N	n.d.
#12	1	Binasal (E-E)	[I] > [C]	N	n.d.
	2	Ipsi-nasal (E-I)	n.d.	n.d.	n.d.
#13	1	Ipsi-nasal (E-0)	n.d.	N	n.d.
	2	n.d.	n.d.	N	n.d.
#14	1	Binasal (E-E)	[I] > [C]	N	n.d.
#15	1	Ipsi-nasal (E-0)	n.d.	n.d.	n.d.
	2	Binasal (E-E)	[I]≒[C]	n.d.	n.d.
	3	Ipsi-nasal (E-0)	n.d.	n.d.	n.d.
	4	Ipsi-nasal (E-0)	n.d.	n.d.	n.d.
#16	1	Binasal (E-E)	[I]≒[C]	n.d.	n.d.
#17	1	Ipsi-nasal (E-0)	n.d.	N	n.d.
	2	Binasal (E-E)	[I] > [C]	n.d.	8
#18	1	Ipsi-nasal (E-I)	n.d.	n.d.	n.d.
	2	Binasal (E-E)	[I] > [C]	N	n.d.
#19	1	Binasal (E-E)	[I] < [C]	n.d.	n.d.
	2	Ipsi-nasal (E-0)	n.d.	n.d.	n.d.
	3	Ipsi-nasal (E-0)	n.d.	n.d.	n.d.
	4	Binasal (E-E)	[I] > [C]	n.d.	n.d.
	5	Binasal (E-E)	[I] > [C]	n.d.	n.d.
	6	Ipsi-nasal (E-0)	n.d.	n.d.	n.d.
#20	1	Binasal (E-E)	[I] > [C]	n.d.	8
	2	Binasal (E-E)	[I]≒[C]	n.d.	6
#21	1	Binasal (E-E)	[I]≒[C]	n.d.	n.d.
#22	1	Ipsi-nasal (E-0)	n.d.	n.d.	n.d.
#23	1	n.d.	n.d.	Y	n.d.

OB neurons

Rats	Cells	E-E, E-0 type
#24	1	Ipsi-nasal (E-0)
	2	Ipsi-nasal (E-0)
	3	Ipsi-nasal (E-0)
	4	Ipsi-nasal (E-0)
	5	Ipsi-nasal (E-0)
	6	Ipsi-nasal (E-0)
	7	Ipsi-nasal (E-0)
#25	1	Ipsi-nasal (E-0)
	2	Ipsi-nasal (E-0)
	3	Ipsi-nasal (E-0)
	4	Ipsi-nasal (E-0)
	5	Ipsi-nasal (E-0)
	6	Ipsi-nasal (E-0)
	7	Ipsi-nasal (E-0)
	8	Ipsi-nasal (E-0)
	9	Ipsi-nasal (E-0)
	10	Ipsi-nasal (E-0)
	11	Ipsi-nasal (E-0)
	12	Ipsi-nasal (E-0)
	13	Ipsi-nasal (E-0)
	14	Ipsi-nasal (E-0)

Y; Yes, N; none, n.d.; not determined

Note: ※1; Averaged magnitude of responses to ipsi-nasal[I] and contra-nasal[C] stimulation.
※2; The boost-up of the responsiveness to contra-nasal odor stimulation after the ipsi-nostril obstruction.
※3; The number of bilateral odorant category matches (among 10 categories).

Table 2

A list of cells that showed resumed respiration phase-locked firing after ipsi-nostril obstruction in each rat

Rats	Cells	Reappearance※1
#26	1	N
#27	1	Y
	2	Y
	3	Y
	4	Y
#28	1	N
	2	Y
	3	N
	4	N
#29	1	Y
	2	N
	3	N
	4	Y
	5	N
	6	N
#30	1	N
	2	N
	3	N
	4	N
	5	N
	6	N
	7	N
	8	N
#31	1	N
	2	N
	3	Y
	4	Y
	5	N
	6	Y
	7	Y
	8	N
	9	Y

Rats	Cells	Reappearance
#32	1	N
	2	Y
	3	Y
	4	N
#33	1	N
	2	N
	3	N
	4	N
	5	N
	6	N
	7	N
	8	N
	9	N
	10	N
	11	Y
	12	N
	13	N
	14	N
	15	N
	16	N
	17	N
	18	N
	19	N
#34	1	N
	2	N
	3	Y
#35	1	N
	2	N
	3	N
	4	Y
	5	N

Note: ※1; Resumed respiration phase-locked firing after ipsi-nostril obstruction
Y; Yes, N; None